1 MitoEAGLE preprint 2018-02-08(22)
2
3 **Mitochondrial respiratory states and rates:**
4 **Building blocks of mitochondrial physiology**
5 **Part 1.**
6 http://www.mitoeagle.org/index.php/MitoEAGLE_preprint_2018-02-08
7 Preprint version 22 (2018-02-08)
8
9 **MitoEAGLE Network**
10 Corresponding author: Gnaiger E
11 Contributing co-authors
12 Ahn B, Alves MG, Amati F, Aral C, Arandarčikaitė O, Åsander Frostner E, Bailey DM,
13 Bastos Sant'Anna Silva AC, Battino M, Beard DA, Ben-Shachar D, Bishop D, Breton S,
14 Brown GC, Brown RA, Buettner GR, Calabria E, Cardoso LHD, Carvalho E, Casado Pinna
15 M, Cervinkova Z, Chang SC, Chicco AJ, Chinopoulos C, Coen PM, Collins JL, Crisóstomo
16 L, Davis MS, Dias T, Distefano G, Doerrier C, Drahota Z, Duchen MR, Ehinger J, Elmer E,
17 Endlicher R, Fell DA, Ferko M, Ferreira JCB, Filipovska A, Fisar Z, Fisher J, Garcia-Roves
18 PM, Garcia-Souza LF, Genova ML, Gonzalo H, Goodpaster BH, Gorr TA, Grefte S, Han J,
19 Harrison DK, Hellgren KT, Hernansanz P, Holland O, Hoppel CL, Houstek J, Hunger M,
20 Iglesias-Gonzalez J, Irving BA, Iyer S, Jackson CB, Jansen-Dürr P, Jespersen NR, Jha RK,
21 Kaambre T, Kane DA, Kappler L, Karabatsiakis A, Keijer J, Keppner G, Komlodi T, Kopitar-
22 Jerala N, Krako Jakovljevic N, Kuang J, Kucera O, Labieniec-Watala M, Lai N, Laner V,
23 Larsen TS, Lee HK, Lemieux H, Lerfall J, Lucchinetti E, MacMillan-Crow LA, Makrecka-
24 Kuka M, Meszaros AT, Michalak S, Moisoi N, Molina AJA, Montaigne D, Moore AL,
25 Moreira BP, Mracek T, Muntane J, Muntean DM, Murray AJ, Nedergaard J, Nemec M,
26 Newsom S, Nozickova K, O'Gorman D, Oliveira PF, Oliveira PJ, Orynbayeva Z, Pak YK,
27 Palmeira CM, Patel HH, Pecina P, Pereira da Silva Grilo da Silva F, Pesta D, Petit PX,
28 Pichaud N, Pirkmajer S, Porter RK, Pranger F, Prochownik EV, Puurand M, Radenkovic F,
29 Reboredo P, Renner-Sattler K, Robinson MM, Rohlena J, Røsland GV, Rossiter HB,
30 Rybacka-Mossakowska J, Salvadego D, Scatena R, Schartner M, Scheibye-Knudsen M,
31 Schilling JM, Schlattner U, Schoenfeld P, Scott GR, Shabalina IG, Shevchuk I, Siewiera K,
32 Singer D, Sobotka O, Spinazzi M, Stankova P, Stier A, Stocker R, Sumbalova Z, Suravajhala
33 P, Tanaka M, Tandler B, Tepp K, Tomar D, Towheed A, Tretter L, Trivigno C, Tronstad KJ,
34 Trougakos IP, Tyrrell DJ, Urban T, Velika B, Vendelin M, Vercesi AE, Victor VM, Villena
35 JA, Wagner BA, Ward ML, Watala C, Wei YH, Wieckowski MR, Wohlwend M, Wolff J,
36 Wuest RCI, Zaugg K, Zaugg M, Zorzano A
37
38 Supporting co-authors:
39 Bakker BM, Bernardi P, Boetker HE, Borsheim E, Borutaitė V, Bouitbir J, Calbet JA, Calzia
40 E, Chaurasia B, Clementi E, Coker RH, Collin A, Das AM, De Palma C, Dubouchaud H,
41 Durham WJ, Dyrstad SE, Engin AB, Fornaro M, Gan Z, Garlid KD, Garten A, Gourlay CW,
42 Granata C, Haas CB, Haavik J, Haendeler J, Hand SC, Hepple RT, Hickey AJ, Hoel F, Jang
43 DH, Kainulainen H, Khamoui AV, Klingenspor M, Koopman WJH, Kowaltowski AJ,
44 Krajcova A, Lane N, Lenaz G, Malik A, Markova M, Mazat JP, Menze MA, Methner A,
45 Neuzil J, Oliveira MT, Pallotta ML, Parajuli N, Pettersen IKN, Porter C, Pulinilkunnil T,
46 Ropelle ER, Salin K, Sandi C, Sazanov LA, Silber AM, Skolik R, Smenes BT, Soares FAA,
47 Sokolova I, Sonkar VK, Swerdlow RH, Szabo I, Trifunovic A, Thyfault JP, Valentine JM,
48 Vieyra A, Votion DM, Williams C, Zischka H
49
50 **Updates and discussion:**
51 http://www.mitoeagle.org/index.php/MitoEAGLE_preprint_2018-02-08

52 Correspondence: Gnaiger E
53 *Department of Visceral, Transplant and Thoracic Surgery, D. Swarovski Research*
54 *Laboratory, Medical University of Innsbruck, Innrain 66/4, A-6020 Innsbruck, Austria*
55 *Email:* erich.gnaiger@i-med.ac.at
56 *Tel: +43 512 566796, Fax: +43 512 566796 20*
57

58 *This manuscript on 'Mitochondrial*
59 *respiratory states and rates' is a position*
60 *statement in the frame of COST Action*
61 *CA15203 MitoEAGLE. The list of co-authors*
62 *evolved beyond* ***phase 1*** *(phase 1 versions 1-*
63 *44) in the* ***bottom-up*** *spirit of COST.*

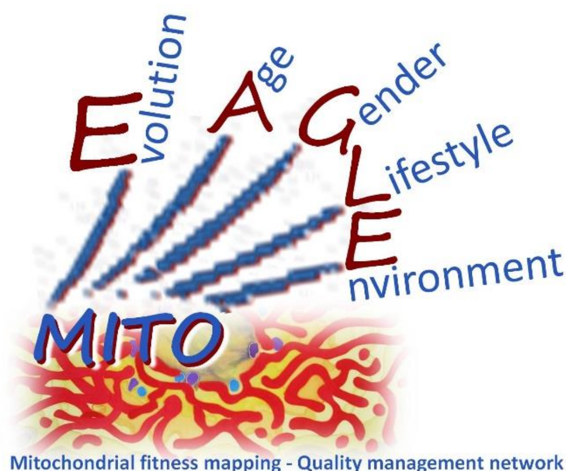

64 *This is an open invitation to scientists*
65 *and students to join as co-authors, to provide*
66 *a balanced view on mitochondrial respiratory*
67 *control, a fundamental introductory*
68 *presentation of the concept of the*
69 *protonmotive force, and a consensus*
70 *statement on reporting data of mitochondrial*
71 *respiration in terms of metabolic flows and*
72 *fluxes.*
73 ***Phase 2:*** *MitoEAGLE preprint 'The protonmotive force and respiratory control'*
74 *(Versions 01 – 21): We continue to invite comments and suggestions, particularly if you are an*
75 ***early career investigator adding an open future-oriented perspective****, or an* ***established***
76 ***scientist providing a balanced historical basis****. Your critical input into the quality of the*
77 *manuscript will be most welcome, improving our aims to be educational, general, consensus-*
78 *oriented, and practically helpful for students working in mitochondrial respiratory physiology.*
79 ***2017-11-11: Print version forMiP2017 and MitoEAGLE workshop in Hradec Kralove****:*
80 » http://www.mitoeagle.org/index.php/MiP2017_Hradec_Kralove_CZ
81 ***Phase 3: Discussion of manuscript submission to a preprint server, such as BioRxiv; invite***
82 ***further opinion leaders:*** *To join as a co-author, please feel free to focus on a particular section*
83 *in terms of direct input and references, contributing to the scope of the manuscript from the*
84 *perspective of your expertise. Your comments will be largely posted on the discussion page of*
85 *the MitoEAGLE preprint website.*
86 *If you prefer to submit comments in the format of a referee's evaluation rather than a*
87 *contribution as a co-author, I will be glad to distribute your views to the updated list of co-*
88 *authors for a balanced response. We would ask for your consent on this open bottom-up policy.*
89 ***Phase 4****: Journal submission. We plan a series of follow-up reports by the expanding*
90 *MitoEAGLE Network, to increase the scope of recommendations on harmonization and*
91 *facilitate global communication and collaboration. Further discussions: MitoEAGLE Working*
92 *Group Meetings, various conferences (EBEC 2018 in Budapest).*
93 » http://www.mitoglobal.org/index.php/EBEC2018_Budapest_HU
94 *I thank you in advance for your feedback.*
95 *With best wishes,*
96
97 *Erich Gnaiger*
98
99 *Chair Mitochondrial Physiology Society* - http://www.mitophysiology.org
100 *Chair COST Action MitoEAGLE* - http://www.mitoeagle.org
101
102

103 **Contents**

104 **1. Introduction** – Box 1: In brief: Mitochondria and Bioblasts
105 **2. Oxidative phosphorylation and coupling states in mitochondrial preparations**
106 Mitochondrial preparations
107 *2.1. Three coupling states of mitochondrial preparations and residual oxygen consumption*
108 Respiratory capacities in coupling control states
109 Kinetic control
110 The steady-state
111 Specification of biochemical dose
112 Phosphorylation, P»
113 Coupling
114 Uncoupling
115 LEAK, OXPHOS, ET, ROX
116 *2.2. Coupling states and respiratory rates*
117 P»/O_2 ratio
118 Control and regulation
119 Respiratory control and response
120 Respiratory coupling control
121 ET-pathway control states
122 *2.3. Classical terminology for isolated mitochondria*
123 States 1-5
124 **3. Normalization: fluxes and flows**
125 *3.1. Normalization: system or sample*
126 Flow per system, I
127 Extensive quantities
128 Size-specific quantities
129 - Box 2: Metabolic fluxes and flows: vectorial and scalar
130 *3.2. Normalization for system-size: flux per chamber volume*
131 System-specific flux, J
132 *3.3. Normalization: per sample*
133 Sample concentration, C_{mX}
134 Mass-specific flux, J_{mX,O_2}
135 Number concentration, C_{NX}
136 Flow per object, I_{X,O_2}
137 *3.4. Normalization for mitochondrial content*
138 Mitochondrial concentration, C_{mtE}, and mitochondrial markers
139 Mitochondria-specific flux, J_{mtE,O_2}
140 *3.5. Evaluation of mitochondrial markers*
141 *3.6. Conversion: units*
142 **4. Conclusions**
143 **5. References** - Box 3: Mitochondrial and cell respiration
144

145
146
147
148
149
150
151
152
153
154
155
156
157
158
159
160
161

Abstract As the knowledge base and importance of mitochondrial physiology to human health expand, the necessity for harmonizing nomenclature concerning mitochondrial respiratory states and rates has become increasingly apparent. Clarity of concept and consistency of nomenclature are key trademarks of a research field. These trademarks facilitate effective transdisciplinary communication, education, and ultimately further discovery. Peter Mitchell's chemiosmotic theory establishes the link between vectorial and scalar energy transformation and coupling in oxidative phosphorylation. The unifying concept of the protonmotive force provides the framework for developing a consistent theory and nomenclature for mitochondrial physiology and bioenergetics. Herein, we follow IUPAC guidelines on general terms of physical chemistry, extended by considerations on open systems and irreversible thermodynamics. We align the nomenclature and symbols of classical bioenergetics with a concept-driven constructive terminology to express the meaning of each quantity clearly and consistently. In this position statement, in the frame of COST Action MitoEAGLE, we endeavour to provide a balanced view on mitochondrial respiratory control and a critical discussion on reporting data of mitochondrial respiration in terms of metabolic flows and fluxes. Uniform standards for evaluation of respiratory states and rates will ultimately support the development of databases of mitochondrial respiratory function in species, tissues, and cells.

162
163
164
165
166

Keywords: Mitochondrial respiratory control, coupling control, mitochondrial preparations, protonmotive force, oxidative phosphorylation, OXPHOS, efficiency, electron transfer, ET; proton leak, LEAK, residual oxygen consumption, ROX, State 2, State 3, State 4, normalization, flow, flux

167
168
169

Executive summary

170
171

In preparation.

172
173
174
175

176
177 **Box 1: In brief – Mitochondria and Bioblasts**
178
179 **Mitochondria** are the oxygen-consuming electrochemical generators which evolved from
180 endosymbiotic bacteria (Margulis 1970; Lane 2005). They were described by Richard Altmann
181 (1894) as 'bioblasts', which include not only the mitochondria as presently defined, but also
182 symbiotic and free-living bacteria. The word 'mitochondria' (Greek mitos: thread; chondros:
183 granule) was introduced by Carl Benda (1898).
184 Mitochondrial dysfunction is associated with a wide variety of genetic and degenerative
185 diseases. Robust mitochondrial function is supported by physical exercise and caloric balance,
186 and is central for sustained metabolic health throughout life. Therefore, a more consistent
187 presentation of mitochondrial physiology will improve our understanding of the etiology of
188 disease, the diagnostic repertoire of mitochondrial medicine, with a focus on protective
189 medicine, lifestyle and healthy aging.
190 We now recognize mitochondria as dynamic organelles with a double membrane that are
191 contained within eukaryotic cells. The mitochondrial inner membrane (mtIM) shows dynamic
192 tubular to disk-shaped cristae that separate the mitochondrial matrix, *i.e.*, the negatively charged
193 internal mitochondrial compartment, and the intermembrane space; the latter being positively
194 charged and enclosed by the mitochondrial outer membrane (mtOM). The mtIM contains the
195 non-bilayer phospholipid cardiolipin, which is not present in any other eukaryotic cellular
196 membrane. Cardiolipin promotes the formation of respiratory supercomplexes, which are
197 supramolecular assemblies based upon specific, though dynamic, interactions between
198 individual respiratory complexes (Greggio *et al.* 2017; Lenaz *et al.* 2017). Membrane fluidity
199 is an important parameter influencing functional properties of proteins incorporated in the
200 membranes (Waczulikova *et al.* 2007).
201 Mitochondria are the structural and functional elements of cell respiration. Cell
202 respiration is the consumption of oxygen by electron transfer coupled to electrochemical proton
203 translocation across the mtIM. In the process of oxidative phosphorylation (OXPHOS), the
204 reduction of O_2 is electrochemically coupled to the transformation of energy in the form of
205 adenosine triphosphate (ATP; Mitchell 1961, 2011). Mitochondria are the powerhouses of the
206 cell which contain the machinery of the OXPHOS-pathways, including transmembrane
207 respiratory complexes (*i.e.*, proton pumps with FMN, Fe-S and cytochrome *b*, *c*, aa_3 redox
208 systems); alternative dehydrogenases and oxidases; the coenzyme ubiquinone (Q); F-ATPase
209 or ATP synthase; the enzymes of the tricarboxylic acid cycle and the fatty acid oxidation
210 enzymes; transporters of ions, metabolites and co-factors; and mitochondrial kinases related to
211 energy transfer pathways. The mitochondrial proteome comprises over 1,200 proteins (Calvo
212 *et al.* 2015; 2017), mostly encoded by nuclear DNA (nDNA), with a variety of functions, many
213 of which are relatively well known (*e.g.* apoptosis-regulating proteins), while others are still
214 under investigation, or need to be identified (*e.g.* alanine transporter).
215 There is a constant crosstalk between mitochondria and the other cellular components,
216 maintaining cellular mitostasis through regulation at both the transcriptional and post-
217 translational level, and through cell signalling including proteostatic (e.g. the ubiquitin-
218 proteasome and autophagy-lysosome pathways) and genome stability modules throughout the
219 cell cycle or even cell death, contributing to homeostatic regulation in response to varying
220 energy demands and stress (Quiros *et al.* 2016). In addition to mitochondrial movement along
221 the microtubules, mitochondrial morphology can change in response to energy requirements of
222 the cell via processes known as fusion and fission, through which mitochondria communicate
223 within a network, and in response to intracellular stress factors causing swelling and ultimately
224 permeability transition.
225 Mitochondria typically maintain several copies of their own genome (hundred to
226 thousands per cell; Cummins 1998), which is maternally inherited (White *et al.* 2008) and

227 known as mitochondrial DNA (mtDNA). One exception to strictly maternal inheritance in
228 animals is found in bivalves (Breton *et al.* 2007). mtDNA is 16.5 kB in length, contains 13
229 protein-coding genes for subunits of the transmembrane respiratory Complexes CI, CIII, CIV
230 and F-ATPase, and also encodes 22 tRNAs and the mitochondrial 16S and 12S rRNA.
231 Additional gene content is encoded in the mitochondrial genome, *e.g.* microRNAs, piRNA,
232 smithRNAs, repeat associated RNA, and even additional proteins (Duarte *et al.* 2014; Lee *et*
233 *al.* 2015; Cobb *et al.* 2016). The mitochondrial genome is both regulated and supplemented by
234 nuclear-encoded mitochondrial targeted proteins.

235 Abbreviation: mt, as generally used in mtDNA. Mitochondrion is singular and
236 mitochondria is plural.

237 '*For the physiologist, mitochondria afforded the first opportunity for an experimental*
238 *approach to structure-function relationships, in particular those involved in active transport,*
239 *vectorial metabolism, and metabolic control mechanisms on a subcellular level*' (Ernster and
240 Schatz 1981).
241

242
243
244 **1. Introduction**
245

246 Mitochondria are the powerhouses of the cell with numerous physiological, molecular,
247 and genetic functions (**Box 1**). Every study of mitochondrial function and disease is faced with
248 **E**volution, **A**ge, **G**ender and sex, **L**ifestyle, and **E**nvironment (EAGLE) as essential background
249 conditions intrinsic to the individual patient or subject, cohort, species, tissue and to some extent
250 even cell line. As a large and highly coordinated group of laboratories and researchers, the
251 mission of the global MitoEAGLE Network is to generate the necessary scale, type, and quality
252 of consistent data sets and conditions to address this intrinsic complexity. Harmonization of
253 experimental protocols and implementation of a quality control and data management system
254 are required to interrelate results gathered across a spectrum of studies and to generate a
255 rigorously monitored database focused on mitochondrial respiratory function. In this way,
256 researchers within the same and across different disciplines will be positioned to compare
257 findings across traditions and generations to an agreed upon set of clearly defined and accepted
258 international standards.

259 Reliability and comparability of quantitative results depend on the accuracy of
260 measurements under strictly-defined conditions. A conceptual framework is required to warrant
261 meaningful interpretation and comparability of experimental outcomes carried out by research
262 groups at different institutes. With an emphasis on quality of research, collected data can be
263 useful far beyond the specific question of a particular experiment. Enabling meta-analytic
264 studies is the most economic way of providing robust answers to biological questions (Cooper
265 *et al.* 2009). Vague or ambiguous jargon can lead to confusion and may relegate valuable
266 signals to wasteful noise. For this reason, measured values must be expressed in standardized
267 units for each parameter used to define mitochondrial respiratory function. Standardization of
268 nomenclature and definition of technical terms are essential to improve the awareness of the
269 intricate meaning of current and past scientific vocabulary, for documentation and integration
270 into databases in general, and quantitative modelling in particular (Beard 2005). The focus on
271 coupling states and fluxes through metabolic pathways of aerobic energy transformation in
272 mitochondrial preparations is a first step in the attempt to generate a harmonized and
273 conceptually-oriented nomenclature in bioenergetics and mitochondrial physiology. Coupling
274 states of intact cells, the protonmotive force, and respiratory control by fuel substrates and
275 specific inhibitors of respiratory enzymes will be reviewed in subsequent communications.
276
277

2. Oxidative phosphorylation and coupling states in mitochondrial preparations

> '*Every professional group develops its own technical jargon for talking about matters of critical concern ... People who know a word can share that idea with other members of their group, and a shared vocabulary is part of the glue that holds people together and allows them to create a shared culture*' (Miller 1991).

Mitochondrial preparations are defined as either isolated mitochondria, or tissue and cellular preparations in which the barrier function of the plasma membrane is disrupted. The plasma membrane separates the cytosol, nucleus, and organelles (the intracellular compartment) from the environment of the cell. The plasma membrane consists of a lipid bilayer, embedded proteins, and attached organic molecules that collectively control the selective permeability of ions, organic molecules, and particles across the cell boundary. The intact plasma membrane, therefore, prevents the passage of many water-soluble mitochondrial substrates, such as succinate or adenosine diphosphate (ADP), that are required for the analysis of respiratory capacity at kinetically-saturating concentrations, thus limiting the scope of investigations into mitochondrial respiratory function in intact cells. The cholesterol content of the plasma membrane is high compared to mitochondrial membranes. Therefore, mild detergents, such as digitonin and saponin, can be applied to selectively permeabilize the plasma membrane by interaction with cholesterol and allow free exchange of cytosolic components with ions and organic molecules of the immediate cell environment, while maintaining the integrity and localization of organelles, cytoskeleton, and the nucleus. Application of optimum concentrations of permeabilization agents (mild detergents or toxins) leads to the complete loss of cell viability, tested by nuclear staining and washout of cytosolic marker enzymes such as lactate dehydrogenase, while mitochondrial function remains intact. The respiration rate of isolated mitochondria remains unaltered after the addition of low concertations of digitonin or saponin. In addition to mechanical permeabilization during homogenization of tissue, peremeabilization agents may be applied to ensure permeabilization of all cells. Suspensions of cells permeabilized in the respiration chamber and crude tissue homogenates contain all components of the cell at highly diluted concentrations. All mitochondria are retained in chemically-permeabilized mitochondrial preparations and crude tissue homogenates. In the preparation of isolated mitochondria, the cells or tissues are homogenized, and the mitochondria are separated from other cell fractions and purified by differential centrifugation, entailing the loss of a fraction of mitochondria. Typical mitochondrial recovery ranges from 30% to 80%. Maximization of the purity of isolated mitochondria may compromise not only the mitochondrial yield but also the structural and functional integrity. Therefore, protocols for isolation of mitochondria need to be optimized according to the relevant questions addressed in a study. The term mitochondrial preparation does not include further fractionation of mitochondrial components, as well as submitochondrial particles.

2.1. Three coupling states of mitochondrial preparations and residual oxygen consumption

Respiratory capacities in coupling control states: To extend the classical nomenclature on mitochondrial coupling states (Section 2.3) by a concept-driven terminology that incorporates explicitly information on the nature of respiratory states, the terminology must be general and not restricted to any particular experimental protocol or mitochondrial preparation (Gnaiger 2009). We focus primarily on the conceptual 'why', along with clarification of the experimental 'how'. In the following section, the concept-driven terminology is explained and coupling states are defined. We define respiratory capacities, comparable to channel capacity in information theory (Schneider 2006), as the upper bound of the rate of respiration measured in defined coupling control states and electron transfer-pathway (ET-pathway) states.

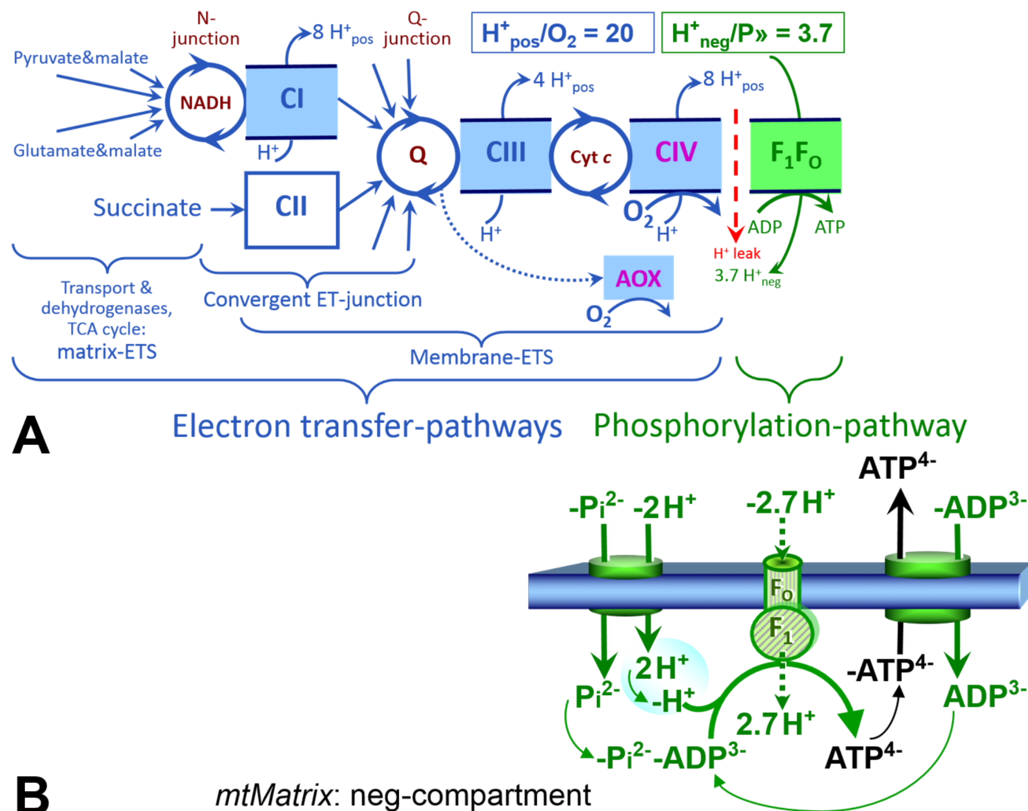

Fig. 1. The oxidative phosphorylation (OXPHOS) system. (A) The mitochondrial electron transfer system (ETS) is fuelled by diffusion and transport of substrates across the mtOM and mtIM and consists of the matrix-ETS and membrane-ETS. Electron transfer (ET) pathways are coupled to the phosphorylation-pathway. ET-pathways converge at the N-junction and Q-junction (additional arrows indicate electron entry into the Q-junction through electron transferring flavoprotein, glycerophosphate dehydrogenase, dihydro-orotate dehydrogenase, choline dehydrogenase, and sulfide-ubiquinone oxidoreductase). The dotted arrow indicates the branched pathway of oxygen consumption by alternative quinol oxidase (AOX). The H^+_{pos}/O_2 ratio is the outward proton flux from the matrix space to the positively (pos) charged compartment, divided by catabolic O_2 flux in the NADH-pathway. The H^+_{neg}/P» ratio is the inward proton flux from the inter-membrane space to the negatively (neg) charged matrix space, divided by the flux of phosphorylation of ADP to ATP (Eq. 1). Due to ion leaks and proton slip these are not fixed stoichiometries. (**B**) Phosphorylation-pathway catalyzed by the proton pump F_1F_O-ATPase, adenine nucleotide translocase, and inorganic phosphate transporter. The H^+_{neg}/P» stoichiometry is the sum of the coupling stoichiometry in the F-ATPase reaction (-2.7 H^+_{pos} from the positive intermembrane space, 2.7 H^+_{neg} to the matrix, *i.e.*, the negative compartment) and the proton balance in the translocation of ADP^{2-}, ATP^{3-} and P_i^{2-}. Modified from (A) Lemieux *et al*. (2017) and (B) Gnaiger (2014).

To provide a diagnostic reference for respiratory capacities of core energy metabolism, the capacity of *oxidative phosphorylation*, OXPHOS, is measured at kinetically-saturating concentrations of ADP and inorganic phosphate, P_i. The *oxidative* ET-capacity reveals the limitation of OXPHOS-capacity mediated by the *phosphorylation*-pathway. The ET- and phosphorylation-pathways comprise coupled segments of the OXPHOS-system. ET-capacity is measured as noncoupled respiration by application of *external uncouplers*. The contribution of *intrinsically uncoupled* oxygen consumption is most easily studied in the absence of ADP, *i.e.*, by not stimulating phosphorylation, or by inhibition of the phosphorylation-pathway. The corresponding states are collectively classified as LEAK-states, when oxygen consumption

357 compensates mainly for ion leaks including the proton leak (**Table 1**). Defined coupling states
358 are induced by: (*1*) adding cation chelators such as EGTA, binding free Ca^{2+} and thus limiting
359 cation cycling; (*2*) adding ADP and P_i; (*3*) inhibiting the phosphorylation-pathway; and (*4*)
360 uncoupler titrations, while maintaining a defined ET-pathway state with constant fuel substrates
361 and inhibitors of specific branches of the ET-pathway (**Fig. 1**).
362
363 **Table 1. Coupling states and residual oxygen consumption in mitochondrial**
364 **preparations in relation to respiration- and phosphorylation-rate, J_{kO_2} and $J_{P»}$,**
365 **and protonmotive force, pmf.** Coupling states are established at kinetically-
366 saturating concentrations of fuel substrates and O_2.

State	J_{kO_2}	$J_{P»}$	pmf	Inducing factors	Limiting factors
LEAK	*L*; low, cation leak-dependent respiration	0	max.	proton leak, slip, and cation cycling	$J_{P»} = 0$: (*1*) without ADP, L_N; (*2*) max. ATP/ADP ratio, L_T; or (*3*) inhibition of the phosphorylation-pathway, L_{Omy}
OXPHOS	*P*; high, ADP-stimulated respiration	max.	high	kinetically-saturating [ADP] and [P_i]	$J_{P»}$ by phosphorylation-pathway; or J_{kO_2} by ET-capacity
ET	*E*; max., noncoupled respiration	0	low	optimal external uncoupler concentration for max. $J_{O_2,E}$	J_{kO_2} by ET-capacity
ROX	*Rox*; min., residual O_2 consumption	0	0	$J_{O_2,Rox}$ in non-ET-pathway oxidation reactions	full inhibition of ET-pathway; or absence of fuel substrates

367
368 **Kinetic control:** Coupling control states are established in the study of mitochondrial
369 preparations to obtain reference values for various output variables. Physiological conditions *in*
370 *vivo* deviate from these experimentally obtained states. Since kinetically-saturating
371 concentrations, *e.g.* of ADP or oxygen, may not apply to physiological intracellular conditions,
372 relevant information is obtained in studies of kinetic responses to conditions intermediate
373 between the LEAK state at zero [ADP] and the OXPHOS-state at saturating [ADP], or of
374 respiratory capacities in the range between kinetically-saturating [O_2] and anoxia (Gnaiger
375 2001).
376 **The steady-state:** Mitochondria represent a thermodynamically open system in non-
377 equilibrium states of biochemical energy transformation. State variables (protonmotive force;
378 redox states) and metabolic *rates* (fluxes) are measured in defined mitochondrial respiratory
379 *states*. Strictly, steady states can be obtained only in open systems, in which changes by *internal*
380 transformations, *e.g.*, O_2 consumption, are instantaneously compensated for by *external* fluxes,
381 *e.g.*, O_2 supply, such that oxygen concentration does not change in the system (Gnaiger 1993b).
382 Mitochondrial respiratory states monitored in closed systems satisfy the criteria of pseudo-
383 steady states for limited periods of time, when changes in the system (concentrations of O_2,
384 fuel substrates, ADP, P_i, H^+) do not exert significant effects on metabolic fluxes (respiration,
385 phosphorylation). Such pseudo-steady states require respiratory media with sufficient buffering
386 capacity and kinetically-saturating concentrations of substrates to be maintained, and thus
387 depend on the kinetics of the processes under investigation.

388 **Specification of biochemical dose:** Substrates, uncouplers, inhibitors, and other
389 biochemical reagents are titrated to dissect mitochondrial function. Nominal concentrations of
390 these substances are usually reported as initial amount of substance concentration [$mol \cdot L^{-1}$] in
391 the incubation medium. When aiming at the measurement of kinetically saturated processes
392 such as OXPHOS-capacities, the concentrations for substrates can be chosen in light of the
393 apparent equilibrium constant, K_m'. In the case of hyperbolic kinetics, only 80% of maximum
394 respiratory capacity is obtained at a substrate concentration of four times the K_m', whereas
395 substrate concentrations of 5, 9, 19 and 49 times the K_m' are theoretically required for reaching
396 83%, 90%, 95% or 98% of the maximal rate (Gnaiger 2001). Other reagents are chosen to
397 inhibit or alter some process. The amount of these chemicals in an experimental incubation is
398 selected to maximize effect, yet not lead to unacceptable off-target consequences that would
399 adversely affect the data being sought. Specifying the amount of substance in an incubation as
400 nominal concentration in the aqueous incubation medium can be ambiguous (Doskey *et al.*
401 2015), particularly when lipophilic substances (oligomycin; uncouplers, permeabilization
402 agents) or cations (TPP^+; fluorescent dyes such as safranin, TMRM) are applied which
403 accumulate in biological membranes or the mitochondrial matrix. For example, a dose of
404 digitonin of 8 $fmol \cdot cell^{-1}$ (10 $\mu g \cdot 10^{-6}$ cells) is optimal for permeabilization of endothelial cells,
405 and the concentration in the incubation medium has to be adjusted according to the cell density
406 applied (Doerrier *et al.* 2018). Generally, dose/exposure can be specified per unit of biological
407 sample, *i.e.*, (nominal moles of xenobiotic)/(number of cells) [$mol \cdot cell^{-1}$] or, as appropriate, per
408 mass of biological sample [$mol \cdot kg^{-1}$]. This approach to specification of dose/exposure provides
409 a scalable parameter that can be used to design experiments, help interpret a wide variety of
410 experimental results, and provide absolute information that allows researchers worldwide to
411 make the most use of published data (Doskey *et al.* 2015).
412 **Phosphorylation, P»:** *Phosphorylation* in the context of OXPHOS is defined as
413 phosphorylation of ADP by P_i to ATP. On the other hand, the term phosphorylation is used
414 generally in many different contexts, *e.g.* protein phosphorylation. This justifies consideration
415 of a symbol more discriminating and specific than P as used in the P/O ratio (phosphate to
416 atomic oxygen ratio; O = 0.5 O_2), where P indicates phosphorylation of ADP to ATP or GDP
417 to GTP. We propose the symbol P» for the endergonic (uphill) direction of phosphorylation
418 ADP→ATP, and likewise the symbol P« for the corresponding exergonic (downhill) hydrolysis
419 ATP→ADP (**Fig. 2**). P» refers mainly to electrontransfer phosphorylation but may also involve
420 substrate-level phosphorylation as part of the tricarboxylic acid cycle (succinyl-CoA ligase)
421 and phosphorylation of ADP catalyzed by phosphoenolpyruvate carboxykinase.
422 Transphosphorylation is performed by adenylate kinase, creatine kinase, hexokinase and
423 nucleoside diphosphate kinase. In isolated mammalian mitochondria ATP production catalyzed
424 by adenylate kinase, 2 ADP ↔ ATP + AMP, proceeds without fuel substrates in the presence
425 of ADP (Komlódi and Tretter 2017). Kinase cycles are involved in intracellular energy transfer
426 and signal transduction for regulation of energy flux.
427 **Coupling:** In mitochondrial electron transfer (**Fig. 1**), vectorial transmembrane proton
428 flux is coupled through the proton pumps CI, CIII and CIV to the catabolic flux of scalar
429 reactions, collectively measured as oxygen flux (**Fig. 2**). Thus mitochondria are important sites
430 of energy transformation. Energy cannot be lost or produced in any internal process (First Law
431 of thermodynamics). Open and closed systems can gain or loose energy only by external fluxes,
432 *i.e.*, by exchange with the environment. Energy is a fundamentally conserved quantity.
433 Therefore, energy can neither be produced by mitochondria, nor is there any internal process
434 without energy conservation. Exergy is defined as the 'free energy' with the potential to
435 perform work. *Coupling* is the mechanistic linkage of an exergonic process (spontaneous,
436 negative exergy change) with an endergonic process (positive exergy change) in energy
437 transformations which conserve part of the exergy that would be irreversible lost or dissipated
438 in an uncoupled process.

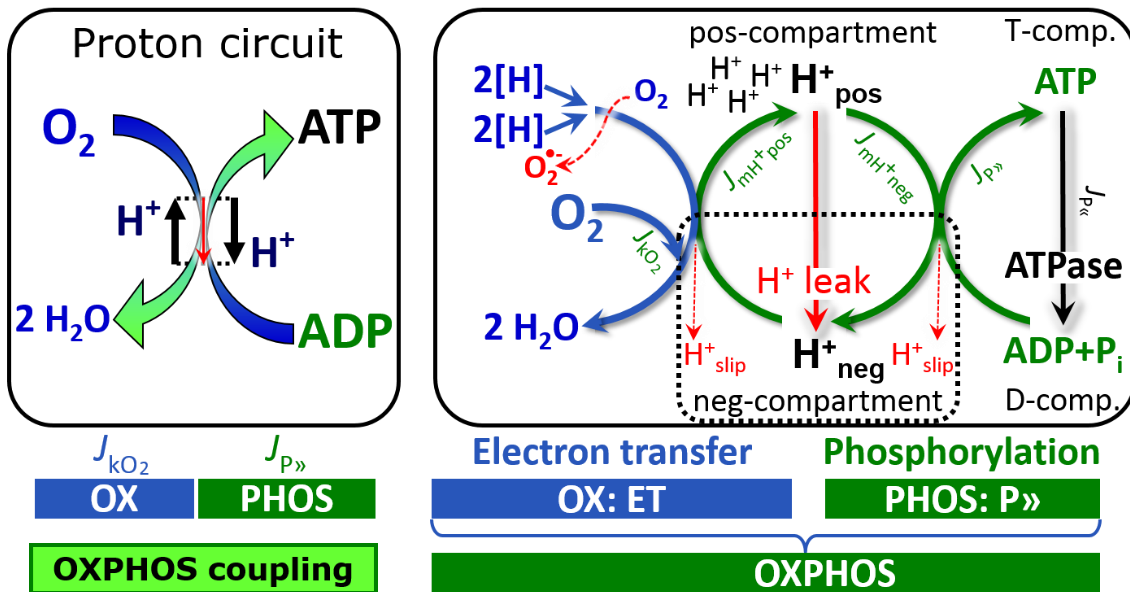

Fig. 2. The proton circuit and coupling in oxidative phosphorylation (OXPHOS). Oxygen flux, J_{kO_2}, through the catabolic ET-pathway, k, is coupled to flux through the phosphorylation-pathway of ADP to ATP, $J_{P»}$. The proton pumps of the ET-pathway drive proton flux into the positive (pos) compartment, J_{mH+pos}, which generates the output protonmotive force. F-ATPase is coupled to inward proton current into the negative (neg) compartment, J_{mH+neg}, to phosphorylate ADP+P$_i$ to ATP. 2[H] indicates the reduced hydrogen equivalents of fuel substrates of the catabolic reaction k with oxygen. Fluxes are expressed per volume, V [m^3], of the system. The system defined by the boundaries (full black line) is not a black box, but is analysed as a compartmental system. The negative compartment (neg-compartment, enclosed by the dotted line) is the matrix space, separated by the mtIM from the positive compartment (pos-compartment). ADP+P$_i$ and ATP are the substrate- and product-compartments (scalar ADP and ATP compartments, D-comp. and T-comp.), respectively. At steady-state proton turnover, $J_{\infty H+}$, and ATP turnover, $J_{\infty P}$, maintain concentrations constant, when $J_{mH+\infty} = J_{mH+pos} = J_{mH+neg}$, and $J_{P\infty} = J_{P»} = J_{P«}$. Modified from Gnaiger (2014).

Uncoupling: Uncoupling is a general term comprising diverse mechanisms. Small differences of terms, *e.g.*, uncoupled *vs.* noncoupled, are easily overlooked, although they relate to different mechanisms of uncoupling (**Fig. 3**). An attempt at rigorous definition is required for clarification of concepts (**Table 2**).

1. Proton leak across the mtIM from the pos- to the neg-compartment (**Fig. 2**);
2. Cycling of other cations, strongly stimulated by permeability transition;
3. Proton slip in the proton pumps when protons are effectively not pumped (CI, CIII and CIV) or are not driving phosphorylation (F-ATPase);
4. Loss of compartmental integrity when electron transfer is acoupled;
5. Electron leak in the loosely coupled univalent reduction of oxygen (O_2; dioxygen) to superoxide anion radical ($O_2^{•-}$).

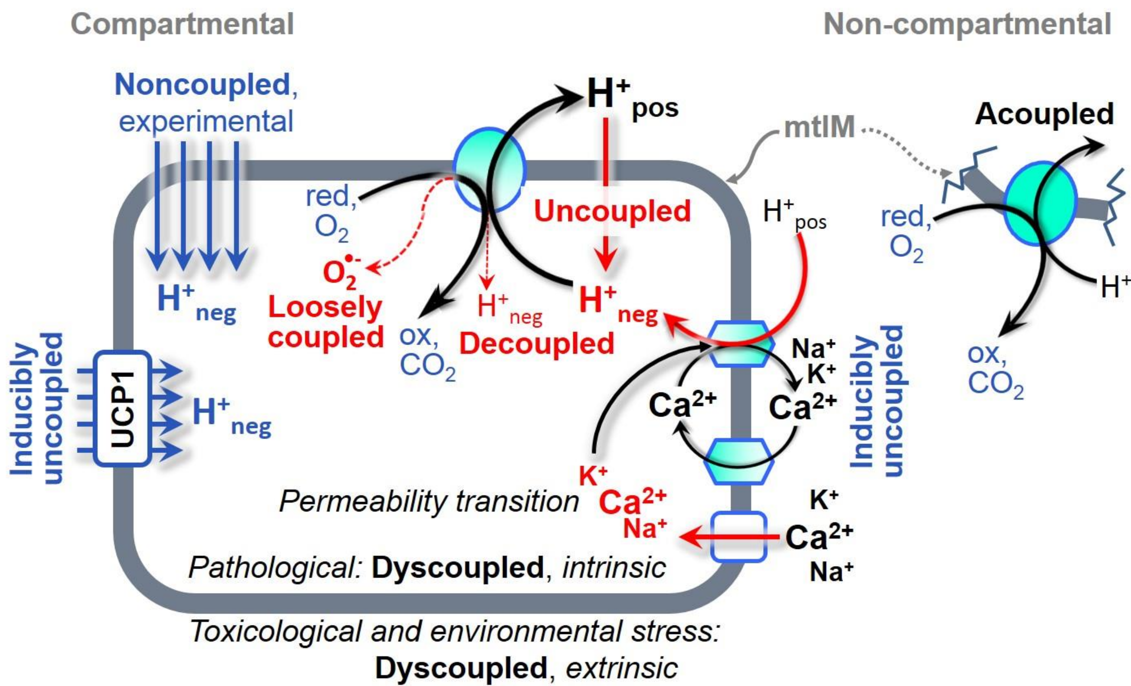

467
468 **Fig 3. Mechanisms of respiratory uncoupling.** An intact mitochondrial inner membrane,
469 mtIM, is required for vectorial, compartmental coupling. 'Acoupled' respiration is the
470 consequence of structural disruption with catalytic activity of non-compartmental
471 mitochondrial fragments. Inducibly uncoupled (activation of UCP1) and experimentally
472 noncoupled respiration (titration of protonophores) stimulate respiration to maximum oxygen
473 flux of ET-capacity. Uncoupled, decoupled, and loosely coupled respiration are components of
474 intrinsic LEAK respiration. Pathological dysfunction may affect all types of uncoupling,
475 including permeability transition, causing intrinsically dyscoupled respiration. Similarly,
476 toxicological and environmental stress factors can cause extrinsically dyscoupled respiration.
477

478 **LEAK-state** (**Fig. 4**): The
479 LEAK-state is defined as a state
480 of mitochondrial respiration
481 when O_2 flux mainly
482 compensates for ion leaks in the
483 absence of ATP synthesis, at
484 kinetically-saturating
485 concentrations of O_2 and
486 respiratory fuel substrates.
487 LEAK-respiration is measured to
488 obtain an estimate of *intrinsic*
489 *uncoupling* without addition of an
490 experimental uncoupler: (*1*) in the
491 absence of adenylates; (*2*) after
492 depletion of ADP at a maximum
493 ATP/ADP ratio; or (*3*) after
494 inhibition of the phosphorylation-
495 pathway by inhibitors of F-
496 ATPase, such as oligomycin, or of adenine nucleotide translocase, such as
497 carboxyatractyloside. It is important to consider adjustment of the nominal concentration of
498 these inhibitors to the density of biological sample applied, to minimize or avoid inhibitory
499 side-effects exerted on ET-capacity or even some dyscoupling.

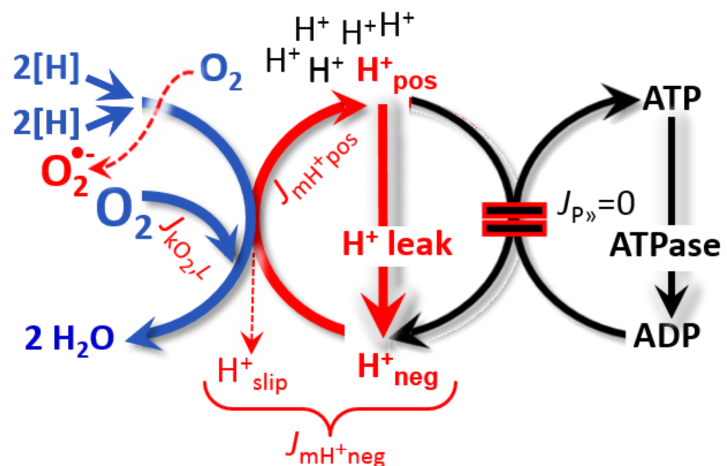

Fig. 4. LEAK-state: Phosphorylation is arrested, $J_{P»} = 0$, and catabolic oxygen flux, $J_{kO_2,L}$, is controlled mainly by the proton leak, $J_{mH+neg,L}$, at maximum protonmotive force. See also **Fig. 2** and **3**.

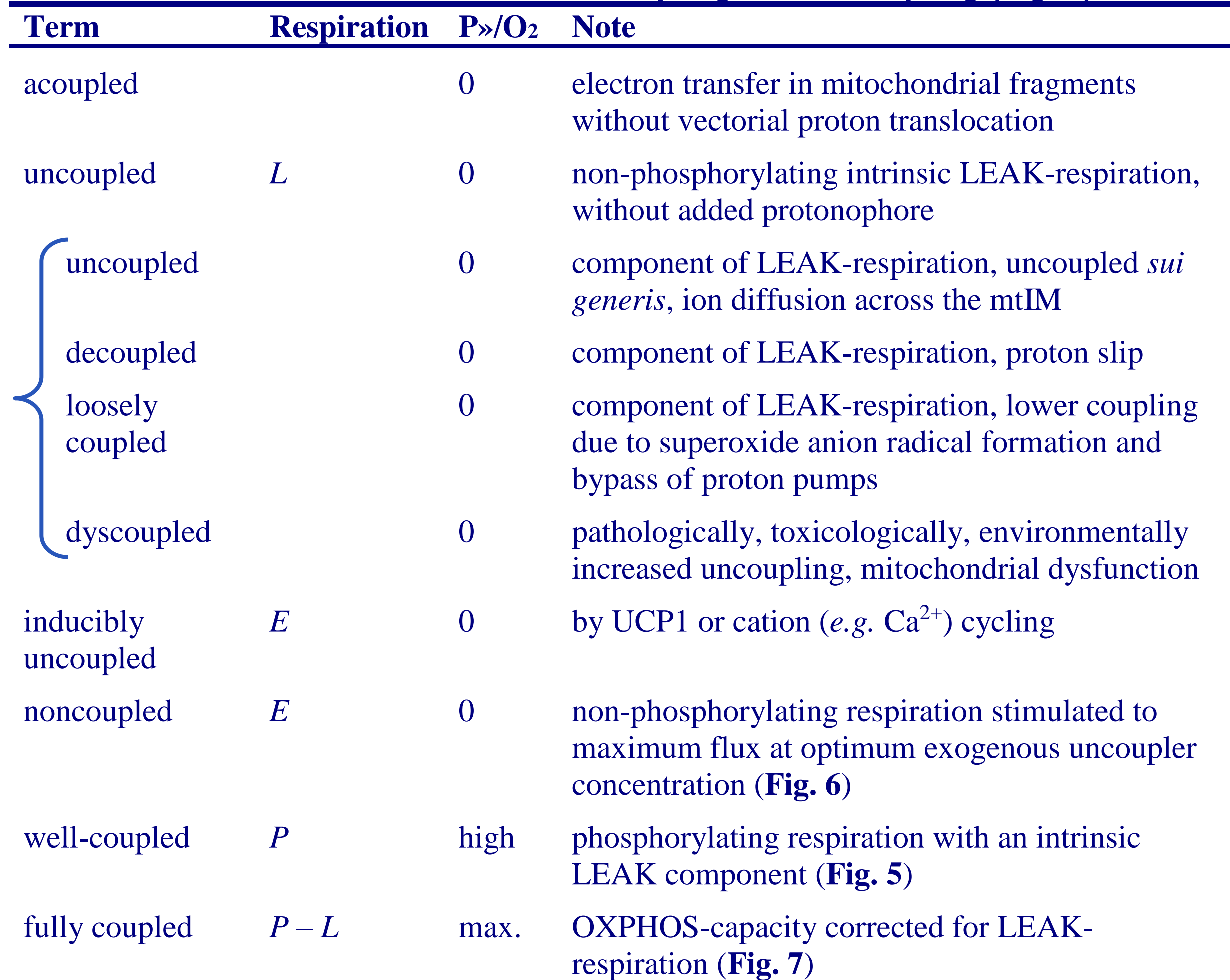

Table 2. Distinction of terms related to coupling and uncoupling (Fig. 3).

Term	Respiration	P»/O2	Note
acoupled		0	electron transfer in mitochondrial fragments without vectorial proton translocation
uncoupled	*L*	0	non-phosphorylating intrinsic LEAK-respiration, without added protonophore
uncoupled		0	component of LEAK-respiration, uncoupled *sui generis*, ion diffusion across the mtIM
decoupled		0	component of LEAK-respiration, proton slip
loosely coupled		0	component of LEAK-respiration, lower coupling due to superoxide anion radical formation and bypass of proton pumps
dyscoupled		0	pathologically, toxicologically, environmentally increased uncoupling, mitochondrial dysfunction
inducibly uncoupled	*E*	0	by UCP1 or cation (*e.g.* Ca^{2+}) cycling
noncoupled	*E*	0	non-phosphorylating respiration stimulated to maximum flux at optimum exogenous uncoupler concentration (**Fig. 6**)
well-coupled	*P*	high	phosphorylating respiration with an intrinsic LEAK component (**Fig. 5**)
fully coupled	*P* – *L*	max.	OXPHOS-capacity corrected for LEAK-respiration (**Fig. 7**)

Proton leak and uncoupled respiration: Proton leak is a leak current of protons. The intrinsic proton leak is the *uncoupled* process in which protons diffuse across the mtIM in the dissipative direction of the downhill protonmotive force without coupling to phosphorylation (**Fig. 4**). The proton leak flux depends non-linearly on the protonmotive force (Garlid *et al.* 1989; Divakaruni and Brand 2011), is a property of the mtIM, and may be enhanced due to possible contaminations by free fatty acids. Inducible uncoupling mediated by uncoupling protein 1 (UCP1) is physiologically controlled, *e.g.*, in brown adipose tissue. UCP1 is a member of the mitochondrial carrier family which is involved in the translocation of protons across the mtIM (Klingenberg 2017). As a consequence of this effective short-circuit, the protonmotive force diminishes, resulting in stimulation of electron transfer to O_2 and heat dissipation without phosphorylation of ADP.

Cation cycling: There can be other cation contributors to leak current including calcium and probably magnesium. Calcium current is balanced by mitochondrial Na^+/Ca^{2+} exchange, which is balanced by Na^+/H^+ exchange or K^+/H^+ exchange. This is another effective uncoupling mechanism different from proton leak.

Proton slip and decoupled respiration: Proton slip is the *decoupled* process in which protons are only partially translocated by a proton pump of the ET-pathways and slip back to the original compartment. The proton leak is the dominant contributor to the overall leak current in mammalian mitochondria incubated under physiological conditions at 37 °C, whereas proton slip is increased at lower experimental temperature (Canton *et al.* 1995). Proton slip can also happen in association with the F-ATPase, in which case the proton slips downhill across the pump to the matrix without contributing to ATP synthesis. In each case, proton slip is a property of the proton pump and increases with the turnover rate of the pump.

525 **Electron leak and loosely coupled respiration**: Superoxide anion radical production by
526 the ETS leads to a bypass of proton pumps and correspondingly lower P»/O_2 ratio, which
527 depends on the actual site of electron leak and the scavenging of hydrogen peroxide by
528 cytochrome *c*, whereby electrons may re-enter the ETS with proton translocation by CIV.
529 **Loss of compartmental integrity and acoupled respiration:** Electron transfer and O_2
530 consumption proceed without compartmental proton translocation in disrupted mitochondrial
531 fragments. Such fragments form during mitochondrial isolation, and may not fully fuse to re-
532 establish structurally intact mitochondria. Loss of mtIM integrity, therefore, is the cause of
533 acoupled respiration, which is a nonvectorial dissipative process without control by the
534 protonmotive force.
535 **Dyscoupled respiration:** Mitochondrial injuries may lead to *dyscoupling* as a
536 pathological or toxicological cause of *uncoupled* respiration. Dyscoupling may involve any
537 type of uncoupling mechanism, *e.g.*, opening the permeability transition pore. Dyscoupled
538 respiration is distinguished from the experimentally induced *noncoupled* respiration in the ET-
539 state (**Fig. 3**).
540
541 **OXPHOS-state** (**Fig. 5**):
542 The OXPHOS-state is defined as
543 the respiratory state with
544 kinetically-saturating
545 concentrations of O_2, respiratory
546 and phosphorylation substrates,
547 and absence of exogenous
548 uncoupler, which provides an
549 estimate of the maximal
550 respiratory capacity in the
551 OXPHOS-state for any given ET-
552 pathway state. Respiratory
553 capacities at kinetically-saturating
554 substrate concentrations provide
555 reference values or upper limits of
556 performance, aiming at the
557 generation of data sets for
558 comparative purposes. Physiological activities and effects of substrate kinetics can be evaluated
559 relative to the OXPHOS-capacity.

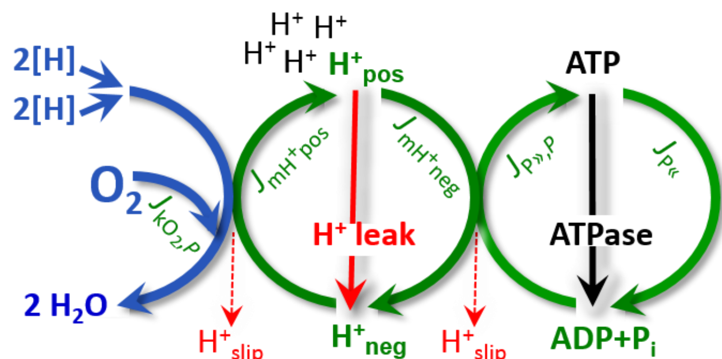

Fig. 5. OXPHOS-state: Phosphorylation, $J_{P»}$, is stimulated by kinetically-saturating [ADP] and inorganic phosphate, [P_i], and is supported by a high protonmotive force. O_2 flux, $J_{kO_2,P}$, is well-coupled at a P»/O_2 ratio of $J_{P»,P}/J_{O_2,P}$. See also **Fig. 2**.

560 As discussed previously, 0.2 mM ADP does not fully saturate flux in isolated
561 mitochondria (Gnaiger 2001; Puchowicz *et al.* 2004); greater ADP concentration is required,
562 particularly in permeabilized muscle fibres and cardiomyocytes, to overcome limitations by
563 intracellular diffusion and by the reduced conductance of the mtOM (Jepihhina *et al.* 2011,
564 Illaste *et al.* 2012, Simson *et al.* 2016), either through interaction with tubulin (Rostovtseva *et*
565 *al.* 2008) or other intracellular structures (Birkedal *et al.* 2014). In permeabilized muscle fibre
566 bundles of high respiratory capacity, the apparent K_m for ADP increases up to 0.5 mM (Saks *et*
567 *al.* 1998), consistent with experimental evidence that >90% saturation is reached only at >5
568 mM ADP (Pesta and Gnaiger 2012). Similar ADP concentrations are also required for accurate
569 determination of OXPHOS-capacity in human clinical cancer samples and permeabilized cells
570 (Klepinin *et al.* 2016; Koit *et al.* 2017). Whereas 2.5 to 5 mM ADP is sufficient to obtain the
571 actual OXPHOS-capacity in many types of permeabilized tissue and cell preparations,
572 experimental validation is required in each specific case.
573

Electron transfer-state (**Fig. 6**): The ET-state is defined as the *noncoupled* state with kinetically-saturating concentrations of O_2, respiratory substrate and optimum *exogenous* uncoupler concentration for maximum O_2 flux, as an estimate of ET-capacity. Inhibition of respiration is observed at higher than optimum uncoupler concentrations. As a consequence of the nearly collapsed protonmotive force, the driving force is insufficient for phosphorylation, and $J_{P»} = 0$.

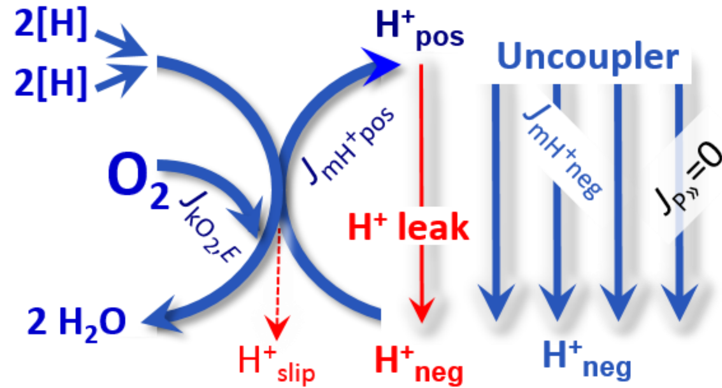

Fig. 6. ET-state: Noncoupled respiration, $J_{kO2,E}$, is maximum at optimum exogenous uncoupler concentration and phosphorylation is zero, $J_{P»} = 0$. See also **Fig. 2**.

Besides the three fundamental coupling states of mitochondrial preparations, the following respiratory state also is relevant to assess respiratory function:

ROX state and *Rox*: The rate of residual oxygen consumption, *Rox*, is defined as O_2 consumption due to oxidative side reactions remaining after inhibition of ET, *e.g.*, with rotenone, malonic acid and antimycin A. Cyanide and azide not only inhibit CIV but several peroxidases which should be involved in *Rox*. ROX is not a coupling state. *Rox* represents a baseline that is used to correct mitochondrial respiration in defined coupling states. *Rox* is not necessarily equivalent to non-mitochondrial respiration, considering oxygen-consuming reactions in mitochondria not related to ET, such as oxygen consumption in reactions catalyzed by monoamine oxidases (type A and B), monooxygenases (cytochrome P450 monooxygenases), dioxygenase (sulfur dioxygenase and trimethyllysine dioxygenase), several hydoxylases, and more. Mitochondrial preparations, especially those obtained from liver, may be contaminated by peroxisomes. This fact makes the exact determination of mitochondrial oxygen consumption and mitochondria-associated generation of reactive oxygen species complicated (Schönfeld *et al.* 2009). The dependence of ROX-linked oxygen consumption needs to be studied in detail with respect to non-ET enzyme activities, availability of specific substrates, oxygen concentration, and electron leakage leading to the formation of reactive oxygen species.

2.2. Coupling states and respiratory rates

As an improvement of previous terminologies, we distinguish metabolic *pathways* from metabolic *states* and the corresponding metabolic *rates*; for example: ET-pathways (**Fig. 7**), ET-state (**Fig. 6**), and ET-capacity, *E*, respectively (**Table 1**). The protonmotive force is *high* in the OXPHOS-state when it drives phosphorylation, *maximum* in the LEAK-state of coupled mitochondria, driven by LEAK-respiration at a minimum back flux of cations to the matrix side, and *very low* in the ET-state when uncouplers short-circuit the proton cycle (**Table 1**).

The three coupling states, ET, LEAK and OXPHOS, are shown schematically with the corresponding respiratory rates, abbreviated as *E*, *L* and *P*, respectively (**Fig. 7**).

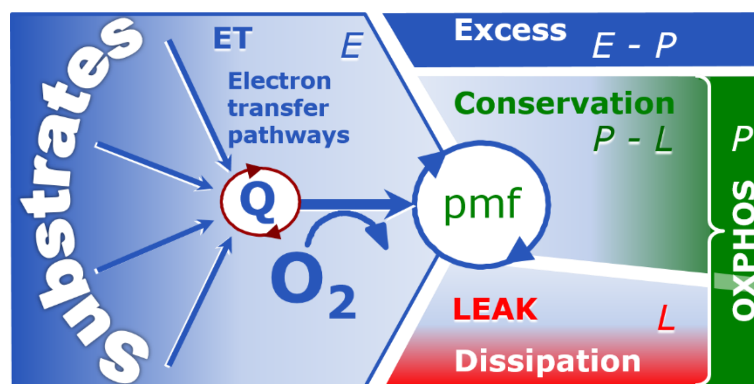

622 **Fig. 7. Four-compartment model of oxidative phosphorylation.** Respiratory states (ET, OXPHOS, LEAK) and corresponding rates (*E, P, L*) are connected by the protonmotive force, pmf. Electron transfer-capacity, *E*, is partitioned into (*1*) dissipative LEAK-respiration, *L*, when the Gibbs energy change of catabolic O_2 consumption is irreversibly lost, (*2*) net OXPHOS-capacity, *P-L*, with partial conservation of the capacity to perform work, and (*3*) the excess capacity, *E-P*. Modified from Gnaiger (2014).

637 *E* may exceed or be equal to *P*. *E* > *P* is observed in many types of mitochondria, varying between species, tissues and cell types (Gnaiger 2009). *E-P* is the excess ET-capacity pushing the phosphorylation-flux (**Fig. 1B**) to the limit of its *capacity of utilizing* the protonmotive force. In addition, the magnitude of *E-P* depends on the tightness of coupling or degree of uncoupling, since an increase of *L* causes *P* to increase towards the limit of *E*. The *excess E-P* capacity, *E-P*, therefore, provides a sensitive diagnostic indicator of specific injuries of the phosphorylation-pathway, under conditions when *E* remains constant but *P* declines relative to controls (**Fig. 7**). Substrate cocktails supporting simultaneous convergent electron transfer to the Q-junction for reconstitution of tricarboxylic acid cycle (TCA cycle or Krebs cycle) function establish pathway control states with high ET-capacity, and consequently increase the sensitivity of the *E-P* assay.

648 *E* cannot theoretically be lower than *P*. *E* < *P* must be discounted as an artefact, which may be caused experimentally by: (*1*) loss of oxidative capacity during the time course of the respirometric assay, since *E* is measured subsequently to *P*; (*2*) using insuffient uncoupler concentrations; (*3*) using high uncoupler concentrations which inhibit ET (Gnaiger 2008); (*4*) high oligomycin concentrations applied for measurement of *L* before titrations of uncoupler, when oligomycin exerts an inhibitory effect on *E*. On the other hand, the excess ET-capacity is overestimated if non-saturating [ADP] or [P_i] are used. See State 3 in the next section.

655 **P»/O_2 ratio:** The P»/O_2 ratio (P»/4 e^-) is two times the 'P/O' ratio (P»/2 e^-) of classical bioenergetics. P»/O_2 is a generalized symbol, independent of measurement of phosphorylation by determination of P_i consumption (P_i/O_2 flux ratio), ADP depletion (ADP/O_2 flux ratio), or ATP production (ATP/O_2 flux ratio).

659 The mechanistic P»/O_2 ratio, which may be referred to also as P»/O_2 stoichiometry, is calculated from the proton-to-oxygen and proton-to-phosphorylation coupling stoichiometries (**Fig. 1A**),

663
$$\mathrm{P»}/\mathrm{O}_2 = \frac{\mathrm{H}^+_{\mathrm{pos}}/\mathrm{O}_2}{\mathrm{H}^+_{\mathrm{neg}}/\mathrm{P»}} \quad (1)$$

665 The H^+_{pos}/O_2 *coupling stoichiometry* (referring to the full 4 electron reduction of O_2) depends on the ET-pathway control state which defines the relative involvement of the three coupling sites (CI, CIII and CIV) in the catabolic pathway of electrons to O_2. This varies with: (*1*) a bypass of CI by single or multiple electron input into the Q-junction; and (*2*) a bypass of CIV by involvement of AOX. H^+_{pos}/O_2 is 12 in the ET-pathways involving CIII and CIV as proton pumps, increasing to 20 for the NADH-pathway (**Fig. 1A**), but a general consensus on H^+_{pos}/O_2 stoichiometries remains to be reached (Hinkle 2005; Wikström and Hummer 2012; Sazanov

672 2015). The H^+_{neg}/P» coupling stoichiometry (3.7; **Fig. 1A**) is the sum of 2.7 H^+_{neg} required by
673 the F-ATPase of vertebrate and most invertebrate species (Watt *et al.* 2010) and the proton
674 balance in the translocation of ADP, ATP and P_i (**Fig. 1B**). Taken together, the mechanistic
675 P»/O_2 ratio is calculated at 5.4 and 3.3 for NADH- and succinate-linked respiration, respectively
676 (Eq. 1). The corresponding classical P»/O ratios (referring to the 2 electron reduction of 0.5 O_2)
677 are 2.7 and 1.6 (Watt *et al.* 2010), in direct agreement with the measured P»/O ratio for succinate
678 of 1.58 ± 0.02 (Gnaiger *et al.* 2000).
679 The effective P»/O_2 flux ratio ($Y_{P»/O_2} = J_{P»}/J_{kO_2}$) is diminished relative to the mechanistic
680 P»/O_2 ratio by intrinsic and extrinsic uncoupling and dyscoupling (**Fig. 3**). Such generalized
681 uncoupling is different from switching to mitochondrial pathways that involve fewer than three
682 proton pumps ('coupling sites': Complexes CI, CIII and CIV), bypassing CI through multiple
683 electron entries into the Q-junction, or CIII and CIV through AOX (**Fig. 1**). Reprogramming of
684 mitochondrial pathways may be considered as a switch of gears (changing the stoichiometry)
685 rather than uncoupling (loosening the stoichiometry). In addition, $Y_{P»/O_2}$ depends on several
686 experimental conditions of flux control, increasing as a hyperbolic function of [ADP] to a
687 maximum value (Gnaiger 2001).
688 The net OXPHOS-capacity is calculated by subtracting *L* from *P* (**Fig. 7**). Then the net
689 P»/O_2 equals P»/(*P-L*), wherein the dissipative LEAK component in the OXPHOS-state may
690 be overestimated. This can be avoided by measuring LEAK-respiration in a state when the
691 protonmotive force is adjusted to its slightly lower value in the OXPHOS-state, *e.g.*, by titration
692 of an ET inhibitor (Divakaruni and Brand 2011). Any turnover-dependent components of
693 proton leak and slip, however, are underestimated under these conditions (Garlid *et al.* 1993).
694 In general, it is inappropriate to use the term *ATP production* or *ATP turnover* for the difference
695 of oxygen consumption measured in states *P* and *L*. The difference *P-L* is the upper limit of the
696 part of OXPHOS-capacity that is freely available for ATP production (corrected for LEAK-
697 respiration) and is fully coupled to phosphorylation with a maximum mechanistic stoichiometry
698 (**Fig. 7**).
699 **Control and regulation:** The terms metabolic *control* and *regulation* are frequently used
700 synonymously, but are distinguished in metabolic control analysis: 'We could understand the
701 regulation as the mechanism that occurs when a system maintains some variable constant over
702 time, in spite of fluctuations in external conditions (homeostasis of the internal state). On the
703 other hand, metabolic control is the power to change the state of the metabolism in response to
704 an external signal' (Fell 1997). Respiratory control may be induced by experimental control
705 signals that *exert* an influence on: (*1*) ATP demand and ADP phosphorylation-rate; (*2*) fuel
706 substrate composition, pathway competition; (*3*) available amounts of substrates and oxygen,
707 *e.g.*, starvation and hypoxia; (*3*) the protonmotive force, redox states, flux-force relationships,
708 coupling and efficiency; (*4*) Ca^{2+} and other ions including H^+; (*5*) inhibitors, *e.g.*, nitric oxide
709 or intermediary metabolites, such as oxaloacetate; (*6*) signalling pathways and regulatory
710 proteins, *e.g.* insulin resistance, transcription factor HIF-1 or inhibitory factor 1. *Mechanisms*
711 of respiratory control and regulation include adjustments of: (*1*) enzyme activities by allosteric
712 mechanisms and phosphorylation; (*2*) enzyme content, concentrations of cofactors and
713 conserved moieties (such as adenylates, nicotinamide adenine dinucleotide [NAD^+/NADH],
714 coenzyme Q, cytochrome *c*); (*3*) metabolic channeling by supercomplexes; and *(4)*
715 mitochondrial density (enzyme concentrations and membrane area) and morphology (cristae
716 folding, fission and fusion). (*5*) Mitochondria are targeted directly by hormones, thereby
717 affecting their energy metabolism (Lee *et al.* 2013; Gerö and Szabo 2016; Price and Dai 2016;
718 Moreno *et al.* 2017). Evolutionary or acquired differences in the genetic and epigenetic basis
719 of mitochondrial function (or dysfunction) between subjects and gene therapy; age; gender,
720 biological sex, and hormone concentrations; life style including exercise and nutrition; and
721 environmental issues including thermal, atmospheric, toxicological and pharmacological

722 factors, exert an influence on all control mechanisms listed above. For reviews, see Brown
723 1992; Gnaiger 1993a, 2009; 2014; Paradies *et al.* 2014; Morrow *et al.* 2017.
724 **Respiratory control and response:** Lack of control by a metabolic pathway, *e.g.*
725 phosphorylation-pathway, does mean that there will be no response to a variable activating it,
726 *e.g.* [ADP]. However, the reverse is not true as the absence of a response to [ADP] does not
727 exclude the phosphorylation-pathway from having some degree of control. The degree of
728 control of a component of the OXPHOS-pathway on an output variable, such as oxygen flux,
729 will in general be different from the degree of control on other outputs, such as phosphorylation-
730 flux or proton leak flux. Therefore, it is necessary to be specific as to which input and output
731 are under consideration (Fell 1997).
732 **Respiratory coupling control:** Respiratory control refers to the ability of mitochondria
733 to adjust oxygen consumption in response to external control signals by engaging various
734 mechanisms of control and regulation. Respiratory control is monitored in a mitochondrial
735 preparation under conditions defined as respiratory states. When phosphorylation of ADP to
736 ATP is stimulated or depressed, an increase or decrease is observed in electron flux linked to
737 oxygen consumption in respiratory coupling states of intact mitochondria (‘controlled states’ in
738 the classical terminology of bioenergetics). Alternatively, coupling of electron transfer with
739 phosphorylation is disengaged by disruption of the integrity of the mtIM or by uncouplers,
740 functioning like a clutch in a mechanical system. The corresponding coupling control state is
741 characterized by high levels of oxygen consumption without control by phosphorylation
742 (‘uncontrolled state’).
743 **ET-pathway control states** are obtained in mitochondrial preparations by depletion of
744 endogenous substrates and addition to the mitochondrial respiration medium of fuel substrates
745 (CHNO; 2[H]) and specific inhibitors, activating selected mitochondrial catabolic pathways, k
746 (**Fig. 1 and 2**). Coupling control states and pathway control states are complementary, since
747 mitochondrial preparations depend on an exogenous supply of pathway-specific fuel substrates
748 and oxygen (Gnaiger 2014).
749
750 *2.3. Classical terminology for isolated mitochondria*
751 *‘When a code is familiar enough, it ceases appearing like a code; one forgets that there*
752 *is a decoding mechanism. The message is identical with its meaning’* (Hofstadter 1979).
753
754 Chance and Williams (1955; 1956) introduced five classical states of mitochondrial respiration
755 and cytochrome redox states. **Table 3** shows a protocol with isolated mitochondria in a closed
756 respirometric chamber, defining a sequence of respiratory states. States and rates are not
757 specifically distinguished in this nomenclature.
758
759 **Table 3. Metabolic states of mitochondria (Chance and**
760 **Williams, 1956; Table V).**
761

State	[O_2]	ADP level	Substrate Level	Respiration rate	Rate-limiting substance
1	>0	low	low	slow	ADP
2	>0	high	~0	slow	substrate
3	>0	high	high	fast	respiratory chain
4	>0	low	high	slow	ADP
5	0	high	high	0	oxygen

762
763 **State 1** is obtained after addition of isolated mitochondria to air-saturated
764 isoosmotic/isotonic respiration medium containing inorganic phosphate, but no fuel substrates
765 and no adenylates, *i.e.*, AMP, ADP, ATP.

766 **State 2** is induced by addition of a 'high' concentration of ADP (typically 100 to 300
767 µM), which stimulates respiration transiently on the basis of endogenous fuel substrates and
768 phosphorylates only a small portion of the added ADP. State 2 is then obtained at a low
769 respiratory activity limited by exhausted endogenous fuel substrate availability (**Table 3**). If
770 addition of specific inhibitors of respiratory complexes, such as rotenone, does not cause a
771 further decline of oxygen consumption, State 2 is equivalent to the state of residual oxygen
772 consumption, ROX (See below.). If inhibition is observed, undefined endogenous fuel
773 substrates are a confounding factor of pathway control, contributing to the effect of
774 subsequently externally added substrates and inhibitors. In contrast to the original protocol, an
775 alternative sequence of titration steps is frequently applied, in which the alternative 'State 2'
776 has an entirely different meaning, when this second state is induced by addition of fuel substrate
777 without ADP (LEAK-state; in contrast to State 2 defined in **Table 1** as a ROX state), followed
778 by addition of ADP.
779 **State 3** is the state stimulated by addition of fuel substrates while the ADP concentration
780 is still high (**Table 3**) and supports coupled energy transformation through oxidative
781 phosphorylation. 'High ADP' is a concentration of ADP specifically selected to allow the
782 measurement of State 3 to State 4 transitions of isolated mitochondria in a closed respirometric
783 chamber. Repeated ADP titration re-establishes State 3 at 'high ADP'. Starting at oxygen
784 concentrations near air-saturation (ca. 200 µM O_2 at sea level and 37 °C), the total ADP
785 concentration added must be low enough (typically 100 to 300 µM) to allow phosphorylation
786 to ATP at a coupled rate of oxygen consumption that does not lead to oxygen depletion during
787 the transition to State 4. In contrast, kinetically-saturating ADP concentrations usually are an
788 order of magnitude higher than 'high ADP', *e.g.* 2.5 mM in isolated mitochondria. The
789 abbreviation State 3u is occasionally used in bioenergetics, to indicate the state of respiration
790 after titration of an uncoupler, without sufficient emphasis on the fundamental difference
791 between OXPHOS-capacity (*well-coupled* with an *endogenous* uncoupled component) and ET-
792 capacity (*noncoupled*).
793 **State 4** is a LEAK-state that is obtained only if the mitochondrial preparation is intact
794 and well-coupled. Depletion of ADP by phosphorylation to ATP leads to a decline in the rate
795 of oxygen consumption in the transition from State 3 to State 4. Under these conditions of State
796 4, a maximum protonmotive force and high ATP/ADP ratio are maintained. For calculation of
797 $P»/O_2$ ratios the gradual decline of $Y_{P»/O_2}$ towards diminishing [ADP] at State 4 must be taken
798 into account (Gnaiger 2001). State 4 respiration, L_T (**Table 1**), reflects intrinsic proton leak and
799 intrinsic ATP hydrolysis activity. Oxygen consumption in State 4 is an overestimation of
800 LEAK-respiration if the contaminating ATP hydrolysis activity recycles some ATP to ADP,
801 $J_{P«}$, which stimulates respiration coupled to phosphorylation, $J_{P»} > 0$. This can be tested by
802 inhibition of the phosphorylation-pathway using oligomycin, ensuring that $J_{P»} = 0$ (State 4o).
803 Alternatively, sequential ADP titrations re-establish State 3, followed by State 3 to State 4
804 transitions while sufficient oxygen is available. However, anoxia may be reached before
805 exhaustion of ADP (State 5).
806 **State 5** is the state after exhaustion of oxygen in a closed respirometric chamber.
807 Diffusion of oxygen from the surroundings into the aqueous solution may be a confounding
808 factor preventing complete anoxia (Gnaiger 2001). Chance and Williams (1955) provide an
809 alternative definition of State 5, which gives it the different meaning of ROX versus anoxia:
810 'State 5 may be obtained by antimycin A treatment or by anaerobiosis'.
811 In **Table 3**, only States 3 and 4 (and 'State 2' in the alternative protocol: addition of fuel
812 substrates without ADP; not included in the table) are coupling control states, with the
813 restriction that O_2 flux in State 3 may be limited kinetically by non-saturating ADP
814 concentrations (**Table 1**).
815
816

817 **3. Normalization: fluxes and flows**

818

819 *3.1. Normalization: system or sample*

820

821 The term *rate* is not sufficiently defined to be useful for a database (**Fig. 8**). The
822 inconsistency of the meanings of rate becomes fully apparent when considering Galileo
823 Galilei's famous principle, that 'bodies of different weight all fall at the same rate (have a
824 constant acceleration)' (Coopersmith 2010).

825

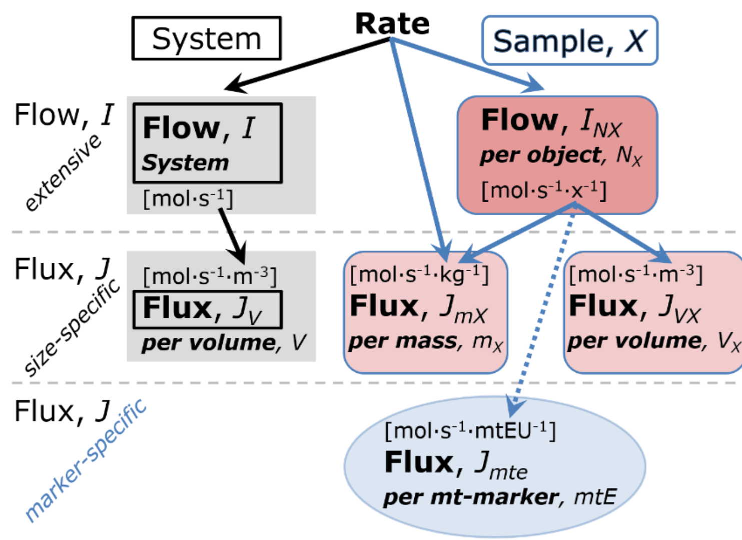

826 **Fig. 8. Different meanings of**
827 ***rate* may lead to confusion, if**
828 **the normalization is not**
829 **sufficiently specified.** Results are
830 frequently expressed as mass-
831 specific *flux*, J_{mX}, per mg protein,
832 dry or wet weight (mass). Cell
833 volume, V_{cell}, may be used for
834 normalization (volume-specific
835 flux, J_{Vcell}), which must be clearly
836 distinguished from flow per cell,
837 I_{Ncell}, or flux, J_V, expressed for
838 methodological reasons per
839 volume of the measurement
840 system. For details see **Table 4**.

841

842 **Flow per system, *I*:** In a generalization of electrical terms, flow as an extensive quantity
843 (per system) is distinguished from flux as a size-specific quantity (per system size) (**Fig. 8**).
844 Electric current is flow, I_{el} [A ≡ C·s^{-1}] per system (extensive quantity). When dividing this
845 extensive quantity by system size (cross-sectional area of a 'wire'), a size-specific quantity is
846 obtained, which is flux (current density), $\boldsymbol{J}_{el}$ [A·m^{-2} = C·s^{-1}·m^{-2}].
847 **Extensive quantities:** An extensive quantity increases proportionally with system size.
848 The magnitude of an extensive quantity is completely additive for non-interacting subsystems,
849 such as mass or flow expressed per defined system. The magnitude of these quantities depends
850 on the extent or size of the system (Cohen *et al.* 2008).
851 **Size-specific quantities:** 'The adjective *specific* before the name of an extensive quantity
852 is often used to mean *divided by mass*' (Cohen *et al.* 2008). In this general system-paradigm,
853 mass-specific flux is flow divided by mass of the *system* (the total mass of everything within
854 the measuring chamber). A mass-specific quantity is independent of the extent of non-
855 interacting homogenous subsystems. Tissue-specific quantities (related to the *sample* in
856 contrast to the *system*) are of fundamental interest in comparative mitochondrial physiology,
857 where *specific* refers to the *type of the sample* rather than *mass of the system*. The term *specific*,
858 therefore, must be further clarified, such that *sample*-specific, *e.g.*, muscle mass-specific
859 normalization is distinguished from *system*-specific (mass or volume) quantities (**Fig. 8**).

860

861 **Box 2: Metabolic fluxes and flows: vectorial and scalar**

862

863 Fluxes are *vectors*, if they have *spatial* direction in addition to magnitude. A vector flux
864 (surface-density of flow) is expressed per unit cross-sectional area, *A* [m^2], perpendicular to the
865 direction of flux. *Flows* are defined as extensive quantities of the *system*, as vector or scalar
866 flow, $\boldsymbol{I}$ or I [mol·s^{-1}], respectively, then the corresponding vector and scalar *fluxes* are $\boldsymbol{J} = \boldsymbol{I}·A^{-1}$
867 [mol·s^{-1}·m^{-2}] and $J = I·V^{-1}$ [mol·s^{-1}·m^{-3}], respectively, expressing flux as an area-specific vector

868 or volume-specific scalar quantity. We suggest to define: (*1*) *vectoral* fluxes, which analyze
869 translocations in continuous systems as functions of gradients; (*2*) *vectorial* fluxes, which
870 describe translocations in discontinuous systems and are restricted to information on
871 compartmental differences (**Fig. 2**, transmembrane proton flux); and (*3*) *scalar* fluxes, which
872 are transformations in a homogenous system (**Fig. 2**, catabolic O_2 flux, J_{kO_2} [mol·s^{-1}·m^{-3}]).
873 Vectorial transmembrane proton fluxes, J_{mH+pos} and J_{mH+neg}, are analyzed in a
874 heterogenous compartmental system as a quantity with *directional* but not *spatial* information.
875 Translocation of protons across the mtIM has a defined direction, either from the negative
876 compartment (matrix space; negative, neg-compartment) to the positive compartment (inter-
877 membrane space; positive, pos-compartment) or *vice versa* (**Fig. 2**). The arrows defining the
878 direction of the translocation between the two compartments may point upwards or downwards,
879 right or left, without any implication that these are actual directions in space. The pos-
880 compartment is neither above nor below the neg-compartment in a spatial sense, but can be
881 visualized arbitrarily in a figure in the upper position (**Fig. 2**). In general, the *compartmental*
882 *direction* of vectorial translocation from the neg-compartment to the pos-compartment is
883 defined by assigning the initial and final state as *ergodynamic compartments*, $H^+_{neg} \rightarrow H^+_{pos}$ or
884 $0 = -1\ H^+_{neg} + 1\ H^+_{pos}$, related to work (erg = work) that must be performed to lift the proton from
885 a lower to a higher electrochemical potential or from the lower to the higher ergodynamic
886 compartment (Gnaiger 1993b).
887 In direct analogy to *vectorial* translocation, the direction of a *scalar* chemical reaction, A
888 → B or 0 = -1 A+1 B, is defined by assigning substrates and products, A and B, as ergodynamic
889 compartments. O_2 is defined as a substrate in respiratory O_2 consumption, which together with
890 the fuel substrates comprises the substrate compartment of the catabolic reaction (**Fig. 2**).
891 Volume-specific scalar O_2 flux is coupled to vectorial translocation, yielding the H^+_{pos}/O_2 ratio
892 (**Fig. 1**).

893
894 *3.2. Normalization for system-size: flux per chamber volume*
895
896 **System-specific flux, *J***: The experimental system (the experimental chamber) is part of
897 the measurement apparatus, separated from the environment as an isolated, closed, open,
898 isothermal or non-isothermal system (**Table 4**). It is important to distinguish between (*1*) the
899 *system* with volume V and mass m defined by the system boundaries, and (*2*) in the experimental
900 chamber enclosed *sample* or *objects* with volume V_X and mass m_X (**Fig. 8**). Metabolic O_2 flow
901 per object, I_{X,O_2}, increases as the mass of the object is increased. Object mass-specific O_2 flux,
902 J_{mX,O_2} should be independent of the mass of the object studied in the instrument chamber, but
903 system volume-specific O_2 flux, J_{V,O_2} (per volume of the instrument chamber), should increase
904 in direct proportion to the mass of the object in the chamber. J_{V,O_2} depends on mass-
905 concentration of the sample in the chamber, but should be independent of the chamber (system)
906 volume. There are practical limitations to increasing the mass-concentration of the sample in
907 the chamber, when one is concerned about crowding effects and instrumental time resolution.
908 When the reactor volume does not change during the reaction, which is typical for liquid
909 phase reactions, the volume-specific *flux of a chemical reaction* r is the time derivative of the
910 advancement of the reaction per unit volume, $J_{V,rB} = d_r\xi_B/dt \cdot V^{-1}$ [(mol·s^{-1})·L^{-1}]. The *rate of*
911 *concentration change* is dc_B/dt [(mol·L^{-1})·s^{-1}], where concentration is $c_B = n_B/V$. It is important
912 to make the fundamental distinction between (*1*) J_{V,rO_2} [mol·s^{-1}·L^{-1}] and (*2*) rate of concentration
913 change [mol·L^{-1}·s^{-1}]. These merge to a single expression only in closed systems. In open
914 systems, external fluxes (such as O_2 supply) are distinguished from internal transformations
915 (metabolic flux, O_2 consumption). In a closed system, external flows of all substances are zero
916 and O_2 consumption (internal flow of catabolic reactions k), I_{kO_2} [pmol·s^{-1}], causes a decline of
917 the amount of O_2 in the system, n_{O_2} [nmol]. Normalization of these quantities for the volume of
918 the system, V [L ≡ dm^3], yields volume-specific O_2 flux, $J_{V,kO_2} = I_{kO_2}/V$ [nmol·s^{-1}·L^{-1}], and O_2

919 concentration, $[O_2]$ or $c_{O_2} = n_{O_2}/V$ [µmol·L^{-1} = µM = nmol·mL^{-1}]. Instrumental background O_2
920 flux is due to external flux into a non-ideal closed respirometer, such that total volume-specific
921 flux has to be corrected for instrumental background O_2 flux, *i.e.*, O_2 diffusion into or out of the
922 instrumental chamber. $J_{V,\mathrm{k}O_2}$ is relevant mainly for methodological reasons and should be
923 compared with the accuracy of instrumental resolution of background-corrected flux, *e.g.*, ±1
924 nmol·s^{-1}·L^{-1} (Gnaiger 2001). 'Metabolic' or catabolic indicates O_2 flux, $J_{\mathrm{k}O_2}$, corrected for: (*1*)
925 instrumental background O_2 flux; (*2*) chemical background O_2 flux due to autoxidation of
926 chemical components added to the incubation medium; and (*3*) *Rox* for O_2-consuming side
927 reactions unrelated to the catabolic pathway k.
928
929 *3.3. Normalization: per sample*
930
931 The challenges of measuring mitochondrial respiratory flux are matched by those of
932 normalization. Application of common and generally defined units is required for direct transfer
933 of reported results into a database. The second [s] is the *SI* unit for the base quantity *time*. It is
934 also the standard time-unit used in solution chemical kinetics. A rate may be considered as the
935 numerator and normalization as the complementary denominator, which are tightly linked in
936 reporting the measurements in a format commensurate with the requirements of a database.
937 Normalization (**Table 4**) is guided by physicochemical principles, methodological
938 considerations (**Fig. 9**), and conceptual strategies (**Fig. 10**).
939
940 **Table 4. Sample concentrations and normalization of flux.**
941

Expression	Symbol	Definition	Unit	Notes
Sample				
identity of sample	X	object: cell, tissue, animal, patient		
number of sample entities X	N_X	number of objects	x	
mass of sample X	m_X		kg	1
mass of object X	M_X	$M_X = m_X \cdot N_X^{-1}$	kg·x^{-1}	1
Mitochondria				
Mitochondria	mt	X = mt		
amount of mt-elements	mtE	quantity of mt-marker	mtEU	
Concentrations				
object number concentration	C_{NX}	$C_{NX} = N_X \cdot V^{-1}$	x·m^{-3}	2
sample mass concentration	C_{mX}	$C_{mX} = m_X \cdot V^{-1}$	kg·m^{-3}	
mitochondrial concentration	C_{mtE}	$C_{mtE} = mtE \cdot V^{-1}$	mtEU·m^{-3}	3
specific mitochondrial density	D_{mtE}	$D_{mtE} = mtE \cdot m_X^{-1}$	mtEU·kg^{-1}	4
mitochondrial content, *mtE* per object *X*	mtE_X	$mtE_X = mtE \cdot N_X^{-1}$	mtEU·x^{-1}	5
O_2 flow and flux				6
flow, system	I_{O_2}	internal flow	mol·s^{-1}	7
volume-specific flux	J_{V,O_2}	$J_{V,O_2} = I_{O_2} \cdot V^{-1}$	mol·s^{-1}·m^{-3}	8
flow per object X	I_{X,O_2}	$I_{X,O_2} = J_{V,O_2} \cdot C_{NX}^{-1}$	mol·s^{-1}·x^{-1}	9
mass-specific flux	J_{mX,O_2}	$J_{mX,O_2} = J_{V,O_2} \cdot C_{mX}^{-1}$	mol·s^{-1}·kg^{-1}	
mitochondria-specific flux	J_{mtE,O_2}	$J_{mtE,O_2} = J_{V,O_2} \cdot C_{mtE}^{-1}$	mol·s^{-1}·mtEU^{-1}	10

1 The *SI* prefix k is used for the SI base unit of mass (kg = 1,000 g). In praxis, various *SI* prefixes are used for convenience, to make numbers easily readable, *e.g.* 1 mg tissue, cell or mitochondrial mass instead of 0.000001 kg.
2 In case sample X = cells, the object number concentration is $C_{N\text{cell}} = N_{\text{cell}} \cdot V^{-1}$, and volume may be expressed in [dm³ ≡ L] or [cm³ = mL]. See **Table 5** for different object types.
3 mt-concentration is an experimental variable, dependent on sample concentration: (*1*) $C_{mtE} = mtE \cdot V^{-1}$; (*2*) $C_{mtE} = mtE_X \cdot C_{NX}$; (*3*) $C_{mtE} = C_{mX} \cdot D_{mtE}$.
4 If the amount of mitochondria, mtE, is expressed as mitochondrial mass, then D_{mtE} is the mass fraction of mitochondria in the sample. If mtE is expressed as mitochondrial volume, V_{mt}, and the mass of sample, m_X, is replaced by volume of sample, V_X, then D_{mtE} is the volume fraction of mitochondria in the sample.
5 $mtE_X = mtE \cdot N_X^{-1} = C_{mtE} \cdot C_{NX}^{-1}$.
6 O_2 can be replaced by other chemicals B to study different reactions, *e.g.* ATP, H_2O_2, or compartmental translocations, *e.g.* Ca^{2+}.
7 I_{O_2} and V are defined per instrument chamber as a system of constant volume (and constant temperature), which may be closed or open. I_{O_2} is abbreviated for $I_{O_2\text{r}}$, *i.e.*, the metabolic or internal O_2 flow of the chemical reaction r in which O_2 is consumed, hence the negative stoichiometric number, $\nu_{O_2} = -1$. $I_{O_2\text{r}} = \text{d}_\text{r}n_{O_2}/\text{d}t \cdot \nu_{O_2}^{-1}$. If r includes all chemical reactions in which O_2 participates, then $\text{d}_\text{r}n_{O_2} = \text{d}n_{O_2} - \text{d}_\text{e}n_{O_2}$, where $\text{d}n_{O_2}$ is the change in the amount of O_2 in the instrument chamber and $\text{d}_\text{e}n_{O_2}$ is the amount of O_2 added externally to the system. At steady state, by definition $\text{d}n_{O_2} = 0$, hence $\text{d}_\text{r}n_{O_2} = -\text{d}_\text{e}n_{O_2}$.
8 J_{V,O_2} is an experimental variable, expressed per volume of the instrument chamber.
9 I_{X,O_2} is a physiological variable, depending on the size of entity X.
10 There are many ways to normalize for a mitochondrial marker, that are used in different experimental approaches: (*1*) $J_{mtE,O_2} = J_{V,O_2} \cdot C_{mtE}^{-1}$; (*2*) $J_{mtE,O_2} = J_{V,O_2} \cdot C_{mX}^{-1} \cdot D_{mtE}^{-1} = J_{mX,O_2} \cdot D_{mtE}^{-1}$; (*3*) $J_{mtE,O_2} = J_{V,O_2} \cdot C_{NX}^{-1} \cdot mtE_X^{-1} = I_{X,O_2} \cdot mtE_X^{-1}$; (*4*) $J_{mtE,O_2} = I_{O_2} \cdot mtE^{-1}$. The mt-elemental unit [mtEU] varies between different mt-markers.

Table 5. Sample types, *X*, abbreviations, and quantification.

Identity of sample mitochondrial preparation	X mtprep	N_X [x]	**Mass**[a] [kg]	**Volume** [m³]	**mt-Marker** [mtEU]
isolated mitochondria	imt		m_{mt}	V_{mt}	mtE
tissue homogenate	thom		m_{thom}		mtE_{thom}
permeabilized tissue	pti		m_{pti}		mtE_{pti}
permeabilized fibre	pfi		m_{pfi}		mtE_{pfi}
permeabilized cell	pce	N_{pce}	M_{pce}	V_{pce}	mtE_{pce}
intact cell	ce	N_{ce}	M_{ce}	V_{ce}	mtE_{ce}
Organism	org	N_{org}	M_{org}	V_{org}	

[a] Instead of mass, frequently the wet weight or dry weight is stated, W_w or W_d. m_X is mass of the sample [kg], M_X is mass of the object [kg·x⁻¹].

Sample concentration, C_{mX}: Normalization for sample concentration is required for reporting respiratory data. Consider a tissue or cells as the sample, X, and the sample mass, m_X [mg] from which a mitochondrial preparation is obtained. m_X is frequently measured as wet or dry weight, W_w or W_d [mg], or as amount of tissue or cell protein, m_{Protein}. In the case of permeabilized tissues, cells, and homogenates, the sample concentration, $C_{mX} = m_X/V$ [mg·mL⁻¹ = g·L⁻¹], is simply the mass of the subsample of tissue that is transferred into the instrument chamber.

Mass-specific flux, J_{mX,O_2}: Mass-specific flux is obtained by expressing respiration per mass of sample, m_X [mg]. X is the type of sample, *e.g.*, tissue homogenate, permeabilized fibres or cells. Volume-specific flux is divided by mass concentration of X, $J_{mX,O_2} = J_{V,O_2}/C_{mX}$; or flow per cell is divided by mass per cell, $J_{m\text{cell},O_2} = I_{\text{cell},O_2}/M_{\text{cell}}$. If mass-specific O_2 flux is constant and independent of sample size (expressed as mass), then there is no interaction between the subsystems. A 1.5 mg and a 3.0 mg muscle sample respires at identical mass-specific flux. Mass-specific O_2 flux, however, may change with the mass of a tissue sample, cells or isolated

988 mitochondria in the measuring chamber, in which case the nature of the interaction becomes an
989 issue. Optimization of cell density and arrangement is generally important and particularly in
990 experiments carried out in wells, considering the confluency of the cell monolayer or clumps
991 of cells (Salabei *et al.* 2014).
992 **Number concentration, C_{NX}:** C_{NX} is the experimental *number concentration* of sample
993 *X*. In the case of cells or animals, *e.g.*, nematodes, $C_{NX} = N_X/V$ [x·L^{-1}], where N_X is the number
994 of cells or organisms in the chamber (**Table 4**).
995 **Flow per object, I_{X,O_2}:** A special case of normalization is encountered in respiratory
996 studies with permeabilized (or intact) cells. If respiration is expressed per cell, the O_2 flow per
997 measurement system is replaced by the O_2 flow per cell, I_{cell,O_2} (**Table 4**). O_2 flow can be
998 calculated from volume-specific O_2 flux, J_{V,O_2} [nmol·s^{-1}·L^{-1}] (per *V* of the measurement chamber
999 [L]), divided by the number concentration of cells, $C_{Nce} = N_{ce}/V$ [cell·L^{-1}], where N_{ce} is the
1000 number of cells in the chamber. Cellular O_2 flow can be compared between cells of identical
1001 size. To take into account changes and differences in cell size, further normalization is required
1002 to obtain cell size-specific or mitochondrial marker-specific O_2 flux (Renner *et al.* 2003).
1003 The complexity changes when the sample is a whole organism studied as an experimental
1004 model. The well-established scaling law in respiratory physiology reveals a strong interaction
1005 of O_2 consumption and individual body mass of an organism, since *basal* metabolic rate (flow)
1006 does not increase linearly with body mass, whereas *maximum* mass-specific O_2 flux, $\dot{V}_{O2max}$ or
1007 $\dot{V}_{O2peak}$, is approximately constant across a large range of individual body mass (Weibel and
1008 Hoppeler 2005), with individuals, breeds, and certain species deviating substantially from this
1009 general relationship. $\dot{V}_{O2peak}$ of human endurance athletes is 60 to 80 mL O_2·min^{-1}·kg^{-1} body
1010 mass, converted to J_{M,O_2peak} of 45 to 60 nmol·s^{-1}·g^{-1} (Gnaiger 2014; **Table 6**).
1011
1012 *3.4. Normalization for mitochondrial content*
1013
1014 Tissues can contain multiple cell populations which may have distinct mitochondrial
1015 subtypes. Mitochondria undergo dynamic fission and fusion cycles, and can exist in multiple
1016 stages and sizes which may be altered by a range of factors. The isolation of mitochondria (often
1017 achieved through differential centrifugation) can therefore yield a subsample of the
1018 mitochondrial types present in a tissue, dependent on isolation protocols utilized (*e.g.*
1019 centrifugation speed). This possible artefact should be taken into account when planning
1020 experiments using isolated mitochondria. The tendency for mitochondria of specific sizes to be
1021 enriched at different centrifugation speeds also has the potential to allow the isolation of specific
1022 mitochondrial subpopulations and therefore the analysis of mitochondria from multiple cell
1023 lineages within a single tissue.
1024 Part of the mitochondria from the tissue is lost during preparation of isolated
1025 mitochondria. The fraction of mitochondria obtained is expressed as mitochondrial recovery
1026 (**Fig. 9**). At a high mitochondrial recovery the sample of isolated mitochondria is more
1027 representative of the total mitochondrial population than in preparations characterized by low
1028 recovery. Determination of the mitochondrial recovery and yield is based on measurement of
1029 the concentration of a mitochondrial marker in the tissue homogenate, $C_{mtE,thom}$, which
1030 simultaneously provides information on the specific mitochondrial density in the sample (**Fig.**
1031 **9**).
1032 Normalization is a problematic subject and it is essential to consider the question of the
1033 study. If the study aims to compare tissue performance, such as the effects of a certain treatment
1034 on a specific tissue, then normalization can be successful, using tissue mass or protein content,
1035 for example. If the aim, however, is to find differences of mitochondrial function independent
1036 of mitochondrial density (**Table 4**), then normalization to a mitochondrial marker is imperative
1037 (**Fig. 10**). However, one cannot assume that quantitative changes in various markers such as
1038 mitochondrial proteins necessarily occur in parallel with one another. It is important to first

establish that the marker chosen is not selectively altered by the performed treatment. In conclusion, the normalization must reflect the question under investigation to reach a satisfying answer. On the other hand, the goal of comparing results across projects and institutions requires some standardization on normalization for entry into a databank.

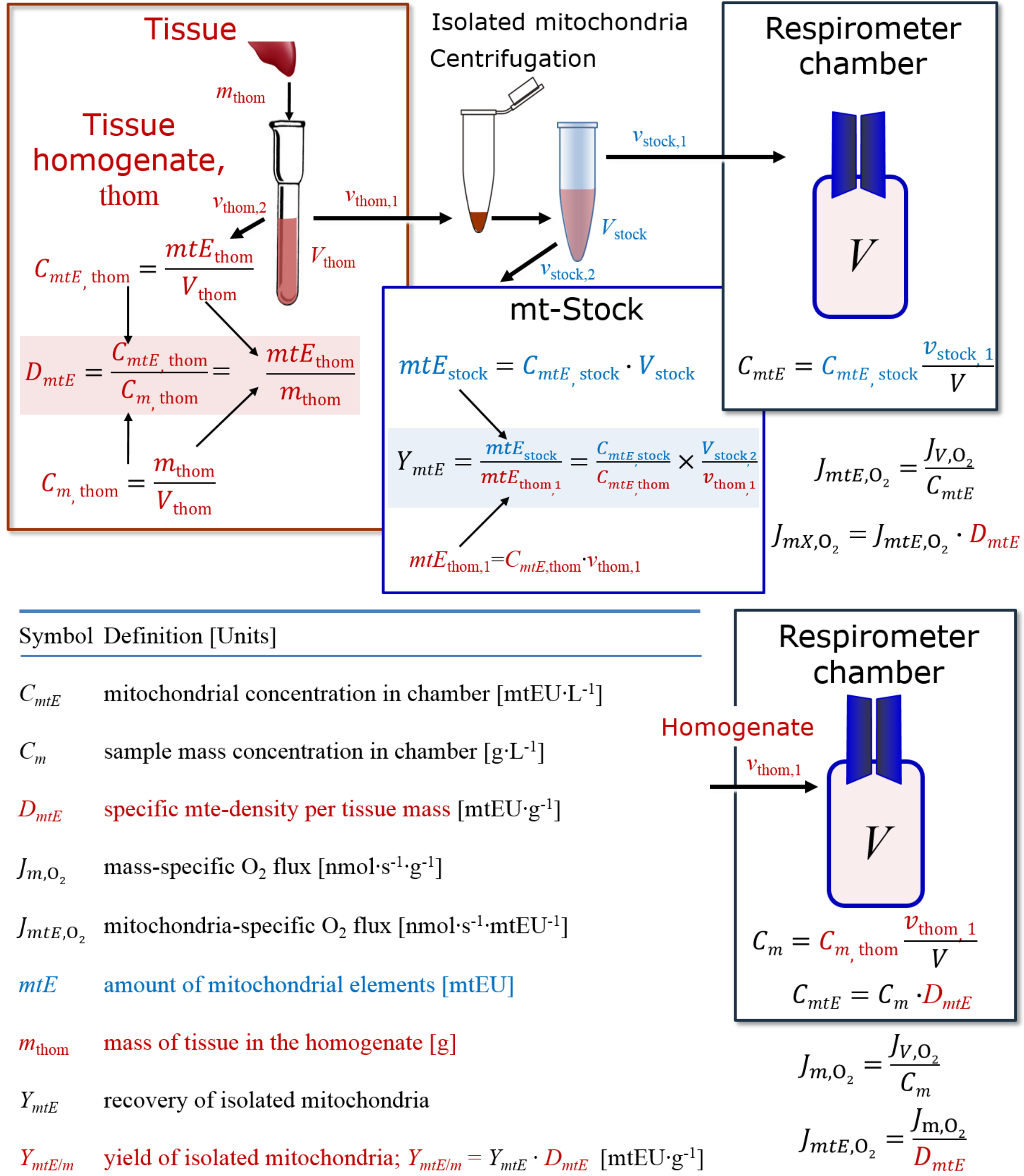

Symbol	Definition [Units]
C_{mtE}	mitochondrial concentration in chamber [mtEU·L^{-1}]
C_m	sample mass concentration in chamber [g·L^{-1}]
D_{mtE}	specific mte-density per tissue mass [mtEU·g^{-1}]
J_{m,O_2}	mass-specific O_2 flux [nmol·s^{-1}·g^{-1}]
J_{mtE,O_2}	mitochondria-specific O_2 flux [nmol·s^{-1}·mtEU^{-1}]
mtE	amount of mitochondrial elements [mtEU]
m_{thom}	mass of tissue in the homogenate [g]
Y_{mtE}	recovery of isolated mitochondria
$Y_{mtE/m}$	yield of isolated mitochondria; $Y_{mtE/m} = Y_{mtE} \cdot D_{mtE}$ [mtEU·g^{-1}]

Fig. 9. Normalization of volume-specific flux of isolated mitochondria and tissue homogenate. A: Recovery, Y_{mtE}, in preparation of isolated mitochondria. $v_{thom,1}$ and $v_{stock,1}$ are the volumes transferred from the total volume, V_{thom} and V_{stock}, respectively. $mtE_{thom,1}$ is the amount of mitochondrial elements in volume $v_{thom,1}$ used for isolation. **B:** Homogenate, $v_{thom,1}$ is transferred directly into the respirometer chamber. See **Table 4** for further symbols.

Mitochondrial concentration, C_{mtE}, and mitochondrial markers: It is important that mitochondrial concentration in the tissue and the measurement chamber be quantified, as a physiological output that is the result of mitochondrial biogenesis and degradation, and as a quantity for normalization in functional analyses. Mitochondrial organelles comprise a dynamic cellular reticulum in various states of fusion and fission. Hence the definition of an "amount" of mitochondria is often misconceived: mitochondria cannot be counted reliably as a number of occurring elements. Therefore, quantification of the "amount" of mitochondria depends on

measurement of chosen mitochondrial markers. ‘Mitochondria are the structural and functional elemental units of cell respiration’ (Gnaiger 2014). The quantity of a mitochondrial marker can be considered to reflect the amount of *mitochondrial elements*, *mtE*, expressed in various mitochondrial elemental units [mtEU] specific for each measured mt-marker (**Table 4**). However, since mitochondrial quality changes under certain stimuli, particularly in mitochondrial dysfunction and after exercise training (Pesta *et al.* 2011; Campos *et al.* 2017), some markers can vary while other markers are unchanged: (*1*) Mitochondrial volume and membrane area are structural markers, whereas mitochondrial protein mass is frequently used as a marker for isolated mitochondria. (*2*) Molecular and enzymatic mitochondrial markers (amounts or activities) can be selected as matrix markers, *e.g.*, citrate synthase activity, mtDNA; mtIM-markers, *e.g.*, cytochrome *c* oxidase activity, aa_3 content, cardiolipin, or mtOM-markers, *e.g.*, TOM20. (*3*) Extending the measurement of mitochondrial marker enzyme activity to mitochondrial pathway capacity, ET- or OXPHOS-capacity can be considered as an integrative functional mitochondrial marker.

Fig. 10. Structure-function analysis of performance of an organism, organ or tissue, or a cell (sample entity, *X*). O_2 flow, I_{X,O_2}, is the product of performance per functional element (element function, mitochondria-specific flux), element density (mitochondrial density, D_{mtE}), and size of entity *X* (mass, M_X). (**A**) Structured analysis: performance is the product of mitochondrial *function* (mt-specific flux) and *structure* (functional elements; D_{mtE} times mass of *X*). (**B**) Unstructured analysis: performance is the product of *entity mass-specific flux*, $J_{mX,O_2} = I_{X,O_2}/M_X = I_{O_2}/m_X$ [mol·s^{-1}·kg^{-1}] and *size of entity*, expressed as mass of *X*; $M_X = m_X{\cdot}N_X^{-1}$ [kg·x^{-1}]. See **Table 4** for further explanation of quantities and units. Modified from Gnaiger (2014).

Depending on the type of mitochondrial marker, the mitochondrial elements, *mtE*, are expressed in marker-specific units. It is recommended to distinguish *experimental mitochondrial concentration*, $C_{mtE} = mtE/V$ and *physiological mitochondrial density*, $D_{mtE} = mtE/m_X$. Then mitochondrial density is the amount of mitochondrial elements per mass of tissue, which is a biological varible (**Fig. 10**). The experimental variable is mitochondrial density multiplied by sample mass concentration in the measuring chamber, $C_{mtE} = D_{mtE}{\cdot}C_{mX}$, or mitochondrial content multiplied by sample number concentration, $C_{mtE} = mtE_X{\cdot}C_{NX}$ (**Table 4**).

1093 **Mitochondria-specific flux, J_{mtE,O_2}**: Volume-specific metabolic O_2 flux depends on: (*1*)
1094 the sample concentration in the volume of the instrument chamber, C_{mX}, or C_{NX}; (*2*) the
1095 mitochondrial density in the sample, $D_{mtE} = mtE/m_X$ or $mtE_X = mtE/N_X$; and (*3*) the specific
1096 mitochondrial activity or performance per elemental mitochondrial unit, $J_{mtE,O_2} = J_{V,O_2}/C_{mtE}$
1097 [$mol \cdot s^{-1} \cdot mtEU^{-1}$] (**Table 4**). Obviously, the numerical results for J_{mtE,O_2} vary according to the
1098 type of mitochondrial marker chosen for measurement of *mtE* and $C_{mtE} = mtE/V$ [$mtEU \cdot m^{-3}$].
1099
1100 *3.5. Evaluation of mitochondrial markers*
1101
1102 Different methods are implicated in quantification of mitochondrial markers and have
1103 different strengths. Some problems are common for all mitochondrial markers, *mtE*: (*1*)
1104 Accuracy of measurement is crucial, since even a highly accurate and reproducible
1105 measurement of O_2 flux results in an inaccurate and noisy expression normalized for a biased
1106 and noisy measurement of a mitochondrial marker. This problem is acute in mitochondrial
1107 respiration because the denominators used (the mitochondrial markers) are often very small
1108 moieties whose accurate and precise determination is difficult. This problem can be avoided
1109 when O_2 fluxes measured in substrate-uncoupler-inhibitor titration protocols are normalized for
1110 flux in a defined respiratory reference state, which is used as an *internal* marker and yields flux
1111 control ratios, *FCR*s (**Fig. 8**). *FCR*s are independent of any *externally* measured markers and,
1112 therefore, are statistically very robust, considering the limitations of ratios in general (Jasienski
1113 and Bazzaz 1999). *FCR*s indicate qualitative changes of mitochondrial respiratory control, with
1114 highest quantitative resolution, separating the effect of mitochondrial density or concentration
1115 on J_{mX,O_2} and I_{X,O_2} from that of function per elemental mitochondrial marker, J_{mtE,O_2} (Pesta *et al.*
1116 2011; Gnaiger 2014). (*2*) If mitochondrial quality does not change and only the amount of
1117 mitochondria varies as a determinant of mass-specific flux, any marker is equally qualified in
1118 principle; then in practice selection of the optimum marker depends only on the accuracy and
1119 precision of measurement of the mitochondrial marker. (*3*) If mitochondrial flux control ratios
1120 change, then there may not be any best mitochondrial marker. In general, measurement of
1121 multiple mitochondrial markers enables a comparison and evaluation of normalization for a
1122 variety of mitochondrial markers. Particularly during postnatal development, the activity of
1123 marker enzymes, such as cytochrome *c* oxidase and citrate synthase, follows different time
1124 courses (Drahota *et al.* 2004). Evaluation of mitochondrial markers in healthy controls is
1125 insufficient for providing guidelines for application in the diagnosis of pathological states and
1126 specific treatments.
1127 In line with the concept of the respiratory control ratio (Chance and Williams 1955a), the
1128 most readily used normalization is that of flux control ratios and flux control factors (Gnaiger
1129 2014). Selection of the state of maximum flux in a protocol as the reference state has the
1130 advantages of: (*1*) internal normalization; (*2*) statistical linearization of the response in the range
1131 of 0 to 1; and (*3*) consideration of maximum flux for integrating a very large number of
1132 elemental steps in the OXPHOS- or ET-pathways. This reduces the risk of selecting a functional
1133 marker that is specifically altered by the treatment or pathodology, yet increases the chance that
1134 the highly integrative pathway is disproportionately affected, *e.g.* the OXPHOS- rather than
1135 ET-pathway in case of an enzymatic defect in the phosphorylation-pathway. In this case,
1136 additional information can be obtained by reporting flux control ratios based on a reference
1137 state which indicates stable tissue-mass specific flux. Stereological determination of
1138 mitochondrial content via two-dimensional transmission electron microscopy can have
1139 limitations due to the dynamics of mitochondrial size (Meinild Lundby *et al.* 2017). Accurate
1140 determination of three-dimensional volume by two-dimensional microscopy can be both time
1141 consuming and statistically challenging (Larsen *et al.* 2012).
1142 The validity of using mitochondrial marker enzymes (citrate synthase activity, Complex
1143 I–IV amount or activity) for normalization of flux is limited in part by the same factors that

apply to flux control ratios. Strong correlations between various mitochondrial markers and citrate synthase activity (Reichmann *et al.* 1985; Boushel *et al.* 2007; Mogensen *et al.* 2007) are expected in a specific tissue of healthy subjects and in disease states not specifically targeting citrate synthase. Citrate synthase activity is acutely modifiable by exercise (Tonkonogi *et al.* 1997; Leek *et al.* 2001). Evaluation of mitochondrial markers related to a selected age and sex cohort cannot be extrapolated to provide recommendations for normalization in respirometric diagnosis of disease, in different states of development and ageing, different cell types, tissues, and species. mtDNA normalised to nDNA via qPCR is correlated to functional mitochondrial markers including OXPHOS- and ET-capacity in some cases (Puntschart *et al.* 1995; Wang *et al.* 1999; Menshikova *et al.* 2006; Boushel *et al.* 2007), but lack of such correlations have been reported (Menshikova *et al.* 2005; Schultz and Wiesner 2000; Pesta *et al.* 2011). Several studies indicate a strong correlation between cardiolipin content and increase in mitochondrial function with exercise (Menshikova *et al.* 2005; Menshikova *et al.* 2007; Larsen *et al.* 2012; Faber *et al.* 2014), but its use as a general mitochondrial biomarker in disease remains questionable.

3.6. Conversion: units

Many different units have been used to report the rate of oxygen consumption, OCR (**Table 6**). *SI* base units provide the common reference for introducing the theoretical principles (**Fig. 8**), and are used with appropriately chosen *SI* prefixes to express numerical data in the most practical format, with an effort towards unification within specific areas of application (**Table 7**). For studies of cells, we recommend that respiration be expressed, as far as possible, as: (*1*) O_2 flux normalized for a mitochondrial marker, for separation of the effects of mitochondrial quality and content on cell respiration (this includes *FCR*s as a normalization for a functional mitochondrial marker); (*2*) O_2 flux in units of cell volume or mass, for comparison of respiration of cells with different cell size (Renner *et al.* 2003) and with studies on tissue preparations, and (*3*) O_2 flow in units of attomole (10^{-18} mol) of O_2 consumed in a second by each cell [$amol \cdot s^{-1} \cdot cell^{-1}$], numerically equivalent to [$pmol \cdot s^{-1} \cdot 10^{-6}$ cells]. This convention allows information to be easily used when designing experiments in which oxygen consumption must be considered. For example, to estimate the volume-specific O_2 flux in an instrument chamber that would be expected at a particular cell number concentration, one simply needs to multiply the flow per cell by the number of cells per volume of interest. This provides the amount of O_2 [mol] consumed per time [s^{-1}] per unit volume [L^{-1}]. At an O_2 flow of 100 $amol \cdot s^{-1} \cdot cell^{-1}$ and a cell density of 10^9 $cells \cdot L^{-1}$ (10^6 $cells \cdot mL^{-1}$), the volume-specific O_2 flux is 100 $nmol \cdot s^{-1} \cdot L^{-1}$ (100 $pmol \cdot s^{-1} \cdot mL^{-1}$).

Although volume is expressed as m^3 using the *SI* base unit, the litre [dm^3] is the basic unit of volume for concentration and is used for most solution chemical kinetics. If one multiplies I_{cell,O_2} by $C_{N\text{cell}}$, then the result will not only be the amount of O_2 [mol] consumed per time [s^{-1}] in one litre [L^{-1}], but also the change in the concentration of oxygen per second (for any volume of an ideally closed system). This is ideal for kinetic modeling as it blends with chemical rate equations where concentrations are typically expressed in $mol \cdot L^{-1}$ (Wagner *et al.* 2011). In studies of multinuclear cells, such as differentiated skeletal muscle cells, it is easy to determine the number of nuclei but not the total number of cells. A generalized concept, therefore, is obtained by substituting cells by nuclei as the sample entity. This does not hold, however, for enucleated platelets.

1193 **Table 6. Conversion of various units used in respirometry and**
1194 **ergometry.** E is the number of electrons or reducing equivalents. z_B is the
1195 charge number of entity B.
1196

1 Unit	x	Multiplication factor	*SI*-unit	Note
ng.atom $O \cdot s^{-1}$	$(2\ e^-)$	0.5	nmol $O_2 \cdot s^{-1}$	
ng.atom $O \cdot min^{-1}$	$(2\ e^-)$	8.33	pmol $O_2 \cdot s^{-1}$	
natom $O \cdot min^{-1}$	$(2\ e^-)$	8.33	pmol $O_2 \cdot s^{-1}$	
nmol $O_2 \cdot min^{-1}$	$(4\ e^-)$	16.67	pmol $O_2 \cdot s^{-1}$	
nmol $O_2 \cdot h^{-1}$	$(4\ e^-)$	0.2778	pmol $O_2 \cdot s^{-1}$	
mL $O_2 \cdot min^{-1}$ at STPD[a]		0.744	µmol $O_2 \cdot s^{-1}$	1
W = J/s at -470 kJ/mol O_2		-2.128	µmol $O_2 \cdot s^{-1}$	
mA = $mC \cdot s^{-1}$	$(z_{H^+} = 1)$	10.36	nmol $H^+ \cdot s^{-1}$	2
mA = $mC \cdot s^{-1}$	$(z_{O_2} = 4)$	2.59	nmol $O_2 \cdot s^{-1}$	2
nmol $H^+ \cdot s^{-1}$	$(z_{H^+} = 1)$	0.09649	mA	3
nmol $O_2 \cdot s^{-1}$	$(z_{O_2} = 4)$	0.38594	mA	3

1197 1 At standard temperature and pressure dry (STPD: 0 °C = 273.15 K and 1 atm =
1198 101.325 kPa = 760 mmHg), the molar volume of an ideal gas, V_m, and V_{m,O_2} is
1199 22.414 and 22.392 $L \cdot mol^{-1}$ respectively. Rounded to three decimal places, both
1200 values yield the conversion factor of 0.744. For comparison at NTPD (20 °C),
1201 V_{m,O_2} is 24.038 $L \cdot mol^{-1}$. Note that the *SI* standard pressure is 100 kPa.
1202 2 The multiplication factor is $10^6/(z_B \cdot F)$.
1203 3 The multiplication factor is $z_B \cdot F/10^6$.
1204
1205
1206 **Table 7. Conversion of units with preservation of numerical values.**

Name	Frequently used unit	Equivalent unit	Note
volume-specific flux, J_{V,O_2}	$pmol \cdot s^{-1} \cdot mL^{-1}$	$nmol \cdot s^{-1} \cdot L^{-1}$	1
	$mmol \cdot s^{-1} \cdot L^{-1}$	$mol \cdot s^{-1} \cdot m^{-3}$	
cell-specific flow, I_{O_2}	$pmol \cdot s^{-1} \cdot 10^{-6}$ cells	$amol \cdot s^{-1} \cdot cell^{-1}$	2
	$pmol \cdot s^{-1} \cdot 10^{-9}$ cells	$zmol \cdot s^{-1} \cdot cell^{-1}$	3
cell number concentration, C_{Nce}	10^6 cells$\cdot mL^{-1}$	10^9 cells$\cdot L^{-1}$	
mitochondrial protein concentration, C_{mtE}	0.1 $mg \cdot mL^{-1}$	0.1 $g \cdot L^{-1}$	
mass-specific flux, J_{m,O_2}	$pmol \cdot s^{-1} \cdot mg^{-1}$	$nmol \cdot s^{-1} \cdot g^{-1}$	4
catabolic power, P_k	$\mu W \cdot 10^{-6}$ cells	$pW \cdot cell^{-1}$	1
volume	1,000 L	m^3 (1,000 kg)	
	L	dm^3 (kg)	
	mL	cm^3 (g)	
	µL	mm^3 (mg)	
	fL	μm^3 (pg)	5
amount of substance concentration	M = $mol \cdot L^{-1}$	$mol \cdot dm^{-3}$	

1207
1208 1 pmol: picomole = 10^{-12} mol
1209 2 amol: attomole = 10^{-18} mol
1210 3 zmol: zeptomole = 10^{-21} mol
4 nmol: nanomole = 10^{-9} mol
5 fL: femtolitre = 10^{-15} L
1211

1212 ET-capacity in various human cell types including HEK 293, primary HUVEC and
1213 fibroblasts ranges from 50 to 180 amol·s^{-1}·cell^{-1}, measured in intact cells in the noncoupled state
1214 (see Gnaiger 2014). At 100 amol·s^{-1}·cell^{-1} corrected for *Rox*, the current across the mt-
1215 membranes, I_{eH+}, approximates 193 pA·cell^{-1} or 0.2 nA per cell. See Rich (2003) for an
1216 extension of quantitative bioenergetics from the molecular to the human scale, with a
1217 transmembrane proton flux equivalent to 520 A in an adult at a catabolic power of -110 W.
1218 Modelling approaches illustrate the link between protonmotive force and currents (Willis *et al.*
1219 2016).
1220 We consider isolated mitochondria as powerhouses and proton pumps as molecular
1221 machines to relate experimental results to energy metabolism of the intact cell. The cellular
1222 P»/O_2 based on oxidation of glycogen is increased by the glycolytic (fermentative) substrate-
1223 level phosphorylation of 3 P»/Glyc, *i.e.*, 0.5 mol P» for each mol O_2 consumed in the complete
1224 oxidation of a mol glycosyl unit (Glyc). Adding 0.5 to the mitochondrial P»/O_2 ratio of 5.4
1225 yields a bioenergetic cell physiological P»/O_2 ratio close to 6. Two NADH equivalents are
1226 formed during glycolysis and transported from the cytosol into the mitochondrial matrix, either
1227 by the malate-aspartate shuttle or by the glycerophosphate shuttle resulting in different
1228 theoretical yields of ATP generated by mitochondria, the energetic cost of which potentially
1229 must be taken into account. Considering also substrate-level phosphorylation in the TCA cycle,
1230 this high P»/O_2 ratio not only reflects proton translocation and OXPHOS studied in isolation,
1231 but integrates mitochondrial physiology with energy transformation in the living cell (Gnaiger
1232 1993a).
1233
1234
1235 **4. Conclusions**
1236
1237 MitoEAGLE can serve as a gateway to better diagnose mitochondrial respiratory defects
1238 linked to genetic variation, age-related health risks, sex-specific mitochondrial performance,
1239 lifestyle with its effects on degenerative diseases, and thermal and chemical environment. The
1240 present recommendations on coupling control states and rates, linked to the concept of the
1241 protonmotive force, are focused on studies with mitochondrial preparations. These will be
1242 extended in a series of reports on pathway control of mitochondrial respiration, respiratory
1243 states in intact cells, and harmonization of experimental procedures.
1244 The optimal choice for expressing mitochondrial and cell respiration (**Box 3**) as O_2 flow
1245 per biological system, and normalization for specific tissue-markers (volume, mass, protein)
1246 and mitochondrial markers (volume, protein, content, mtDNA, activity of marker enzymes,
1247 respiratory reference state) is guided by the scientific question under study. Interpretation of
1248 the obtained data depends critically on appropriate normalization, and therefore reporting rates
1249 merely as nmol·s^{-1} is discouraged, since it restricts the analysis to intra-experimental
1250 comparison of relative (qualitative) differences. Expressing O_2 consumption per cell may not
1251 be possible when dealing with tissues. For studies with mitochondrial preparations, we
1252 recommend that normalizations be provided as far as possible: (*1*) on a per cell basis as O_2 flow
1253 (a biophysical normalization); (*2*) per g cell or tissue protein, or per cell or tissue mass as mass-
1254 specific O_2 flux (a cellular normalization); and (*3*) per mitochondrial marker as mt-specific flux
1255 (a mitochondrial normalization). With information on cell size and the use of multiple
1256 normalizations, maximum potential information is available (Renner *et al.* 2003; Wagner *et al.*
1257 2011; Gnaiger 2014).
1258 When using isolated mitochondria, mitochondrial protein is a frequently applied
1259 mitochondrial marker, the use of which is basically restricted to isolated mitochondria. The
1260 mitochondrial recovery and yield, and experimental criteria for evaluation of purity versus
1261 integrity should be reported. Mitochondrial markers, such as citrate synthase activity as an
1262 enzymatic matrix marker, provide a link to the tissue of origin on the basis of calculating the

mitochondrial recovery, *i.e.*, the fraction of mitochondrial marker obtained from a unit mass of tissue.

Table 8. Terms, symbols, and units.

Term	Symbol	*SI* unit	Links and comments
alternative quinol oxidase	AOX		Fig. 1
amount of substance B	n_B	[mol]	
apparent equilibrium constant	K_m'		
Complexes I to IV	CI to CIV		respiratory ET Complexes; Fig. 1
concentration of substance B	$c_B = n_B \cdot V^{-1}$; [B]	[mol·m^{-3}]	Box 2
electron transfer system	ETS		
flow, for substance B	I_B	[mol·s^{-1}]	system-related extensive quantity; Fig. 8
flux, for substance B	J_B	*varies*	size-specific quantitiy; Fig. 8
inorganic phosphate	P_i		
LEAK	LEAK		Tab. 1
mass of sample *X*	m_X	[kg]	Tab. 4
mass of entity *X*	M_X	[kg]	Tab. 4
MITOCARTA			https://www.broadinstitute.org/scientific-community/science/programs/metabolic-disease-program/publications/mitocarta/mitocarta-in-0
mitochondria or mitochondrial	mt		Box 1
mitochondrial DNA	mtDNA		Box 1
mitochondrial concentration	$C_{mtE} = mtE \cdot V^{-1}$	[mtEU·m^{-3}]	Tab. 4
mitochondrial content	$mtE_X = mtE \cdot N_X^{-1}$	[mtEU·x^{-1}]	Tab. 4
mitochondrial elemental unit	mtEU	*varies*	Tab. 4, specific units for mt-marker
mitochondrial inner membrane	mtIM		MIM is widely used, and M is replaced by mt as abbreviation for mitochondria; Box 1
mitochondrial outer membrane	mtOM		MOM is widely used, and M is replaced by mt as abbreviation for mitochondria; Box 1
mitochondrial recovery	Y_{mtE}		Fig. 9
mitochondrial yield	$Y_{mtE/m}$		Fig. 9
negative	neg		Fig. 2
number concentration of *X*	C_{NX}	[x·m^{-3}]	Tab. 4
number of entities *X*	N_X	[x]	Tab. 4, Fig. 10
number of entity B	N_B	[x]	Tab. 4
oxidative phosphorylation	OXPHOS		Tab. 1
oxygen concentration	$c_{O2} = n_{O2} \cdot V^{-1}$; [$O_2$]	[mol·m^{-3}]	Section 3.2
phosphorylation of ADP to ATP	P»		Section 2.2
positive	pos		Fig. 2
proton in the negative compartment	H^+_{neg}		Fig. 2
proton in the positive compartment	H^+_{pos}		Fig. 2
rate of electron transfer in ET state	*E*		ET-capacity; Tab. 1
rate of LEAK respiration	*L*		Tab. 1
rate of oxidative phosphorylation	*P*		OXPHOS capacity; Tab. 1
rate of residual oxygen consumption	*Rox*		Tab. 1
residual oxygen consumption	ROX		Tab. 1
specific mitochondrial density	$D_{mtE} = mtE \cdot m_X^{-1}$	[mtEU·kg^{-1}]	Tab. 7
volume	*V*	[m^{-3}]	
weight, dry weight	W_d	[kg]	used as mass of sample *X*; Fig. 8
weight, wet weight	W_w	[kg]	used as mass of sample *X*; Fig. 8

Terms and symbols are summarized in **Table 8**. Their use will facilitate transdisciplinary communication and support further developments towards a consistent theory of bioenergetics and mitochondrial physiology.

Box 3: Mitochondrial and cell respiration

Mitochondrial and cell respiration is the process of highly exergonic and exothermic energy transformation in which scalar redox reactions are coupled to vectorial ion translocation across a semipermeable membrane, which separates the small volume of a bacterial cell or mitochondrion from the larger volume of its surroundings. The electrochemical exergy can be partially conserved in the phosphorylation of ADP to ATP or in ion pumping, or dissipated in an electrochemical short-circuit. Respiration is thus clearly distinguished from fermentation as the counterpart of cellular core energy metabolism. Respiration is separated in mitochondrial preparations from the partial contribution of fermentative pathways of the intact cell. According to this definition, residual oxygen consumption, as measured after inhibition of mitochondrial electron transfer, does not belong to the class of catabolic reactions and is, therefore, subtracted from total oxygen consumption to obtain baseline-corrected respiration.

Acknowledgements

We thank M. Beno for management assistance. Supported by COST Action CA15203 MitoEAGLE and K-Regio project MitoFit (E.G.).

Competing financial interests: E.G. is founder and CEO of Oroboros Instruments, Innsbruck, Austria.

5. References

Altmann R (1894) Die Elementarorganismen und ihre Beziehungen zu den Zellen. Zweite vermehrte Auflage. Verlag Von Veit & Comp, Leipzig:160 pp.

Beard DA (2005) A biophysical model of the mitochondrial respiratory system and oxidative phosphorylation. PLoS Comput Biol 1(4):e36.

Benda C (1898) Weitere Mitteilungen über die Mitochondria. Verh Dtsch Physiol Ges:376-83.

Birkedal R, Laasmaa M, Vendelin M (2014) The location of energetic compartments affects energetic communication in cardiomyocytes. Front Physiol 5:376.

Breton S, Beaupré HD, Stewart DT, Hoeh WR, Blier PU (2007) The unusual system of doubly uniparental inheritance of mtDNA: isn't one enough? Trends Genet 23:465-74.

Brown GC (1992) Control of respiration and ATP synthesis in mammalian mitochondria and cells. Biochem J 284:1-13.

Calvo SE, Klauser CR, Mootha VK (2016) MitoCarta2.0: an updated inventory of mammalian mitochondrial proteins. Nucleic Acids Research 44:D1251-7.

Calvo SE, Julien O, Clauser KR, Shen H, Kamer KJ, Wells JA, Mootha VK (2017) Comparative analysis of mitochondrial N-termini from mouse, human, and yeast. Mol Cell Proteomics 16:512-23.

Campos JC, Queliconi BB, Bozi LHM, Bechara LRG, Dourado PMM, Andres AM, Jannig PR, Gomes KMS, Zambelli VO, Rocha-Resende C, Guatimosim S, Brum PC, Mochly-Rosen D, Gottlieb RA, Kowaltowski AJ, Ferreira JCB (2017) Exercise reestablishes autophagic flux and mitochondrial quality control in heart failure. Autophagy 13:1304-317.

Canton M, Luvisetto S, Schmehl I, Azzone GF (1995) The nature of mitochondrial respiration and discrimination between membrane and pump properties. Biochem J 310:477-81.

Chance B, Williams GR (1955a) Respiratory enzymes in oxidative phosphorylation. I. Kinetics of oxygen utilization. J Biol Chem 217:383-93.

Chance B, Williams GR (1955b) Respiratory enzymes in oxidative phosphorylation: III. The steady state. J Biol Chem 217:409-27.

Chance B, Williams GR (1955c) Respiratory enzymes in oxidative phosphorylation. IV. The respiratory chain. J Biol Chem 217:429-38.

Chance B, Williams GR (1956) The respiratory chain and oxidative phosphorylation. Adv Enzymol Relat Subj Biochem 17:65-134.

1379 Cobb LJ, Lee C, Xiao J, Yen K, Wong RG, Nakamura HK, Mehta HH, Gao Q, Ashur C, Huffman DM, Wan J,
1380 Muzumdar R, Barzilai N, Cohen P (2016) Naturally occurring mitochondrial-derived peptides are age-
1381 dependent regulators of apoptosis, insulin sensitivity, and inflammatory markers. Aging (Albany NY) 8:796-
1382 809.
1383 Cohen ER, Cvitas T, Frey JG, Holmström B, Kuchitsu K, Marquardt R, Mills I, Pavese F, Quack M, Stohner J,
1384 Strauss HL, Takami M, Thor HL (2008) Quantities, units and smbols in physical chemistry, IUPAC Green
1385 Book, 3rd Edition, 2nd Printing, IUPAC & RSC Publishing, Cambridge.
1386 Cooper H, Hedges LV, Valentine JC, eds (2009) The handbook of research synthesis and meta-analysis. Russell
1387 Sage Foundation.
1388 Coopersmith J (2010) Energy, the subtle concept. The discovery of Feynman's blocks from Leibnitz to Einstein.
1389 Oxford University Press:400 pp.
1390 Cummins J (1998) Mitochondrial DNA in mammalian reproduction. Rev Reprod 3:172-82.
1391 Dai Q, Shah AA, Garde RV, Yonish BA, Zhang L, Medvitz NA, Miller SE, Hansen EL, Dunn CN, Price TM
1392 (2013) A truncated progesterone receptor (PR-M) localizes to the mitochondrion and controls cellular
1393 respiration. Mol Endocrinol 27:741-53.
1394 Divakaruni AS, Brand MD (2011) The regulation and physiology of mitochondrial proton leak. Physiology
1395 (Bethesda) 26:192-205.
1396 Doerrier C, Garcia-Souza LF, Krumschnabel G, Wohlfarter Y, Mészáros AT, Gnaiger E (2018) High-Resolution
1397 FluoRespirometry and OXPHOS protocols for human cells, permeabilized fibres from small biopsies of
1398 muscle and isolated mitochondria. Methods Mol. Biol. (in press)
1399 Doskey CM, van 't Erve TJ, Wagner BA, Buettner GR (2015) Moles of a substance per cell is a highly
1400 informative dosing metric in cell culture. PLOS ONE 10:e0132572.
1401 Drahota Z, Milerová M, Stieglerová A, Houstek J, Ostádal B (2004) Developmental changes of cytochrome *c*
1402 oxidase and citrate synthase in rat heart homogenate. Physiol Res 53:119-22.
1403 Duarte FV, Palmeira CM, Rolo AP (2014) The role of microRNAs in mitochondria: small players acting wide.
1404 Genes (Basel) 5:865-86.
1405 Ernster L, Schatz G (1981) Mitochondria: a historical review. J Cell Biol 91:227s-55s.
1406 Estabrook RW (1967) Mitochondrial respiratory control and the polarographic measurement of ADP:O ratios.
1407 Methods Enzymol 10:41-7.
1408 Faber C, Zhu ZJ, Castellino S, Wagner DS, Brown RH, Peterson RA, Gates L, Barton J, Bickett M, Hagerty L,
1409 Kimbrough C, Sola M, Bailey D, Jordan H, Elangbam CS (2014) Cardiolipin profiles as a potential
1410 biomarker of mitochondrial health in diet-induced obese mice subjected to exercise, diet-restriction and
1411 ephedrine treatment. J Appl Toxicol 34:1122-9.
1412 Fell D (1997) Understanding the control of metabolism. Portland Press.
1413 Garlid KD, Beavis AD, Ratkje SK (1989) On the nature of ion leaks in energy-transducing membranes. Biochim
1414 Biophys Acta 976:109-20.
1415 Garlid KD, Semrad C, Zinchenko V. Does redox slip contribute significantly to mitochondrial respiration? In:
1416 Schuster S, Rigoulet M, Ouhabi R, Mazat J-P, eds (1993) Modern trends in biothermokinetics. Plenum Press,
1417 New York, London:287-93.
1418 Gerö D, Szabo C (2016) Glucocorticoids suppress mitochondrial oxidant production via upregulation of
1419 uncoupling protein 2 in hyperglycemic endothelial cells. PLoS One 11:e0154813.
1420 Gnaiger E. Efficiency and power strategies under hypoxia. Is low efficiency at high glycolytic ATP production a
1421 paradox? In: Surviving Hypoxia: Mechanisms of Control and Adaptation. Hochachka PW, Lutz PL, Sick T,
1422 Rosenthal M, Van den Thillart G, eds (1993a) CRC Press, Boca Raton, Ann Arbor, London, Tokyo:77-109.
1423 Gnaiger E (1993b) Nonequilibrium thermodynamics of energy transformations. Pure Appl Chem 65:1983-2002.
1424 Gnaiger E (2001) Bioenergetics at low oxygen: dependence of respiration and phosphorylation on oxygen and
1425 adenosine diphosphate supply. Respir Physiol 128:277-97.
1426 Gnaiger E (2009) Capacity of oxidative phosphorylation in human skeletal muscle. New perspectives of
1427 mitochondrial physiology. Int J Biochem Cell Biol 41:1837-45.
1428 Gnaiger E (2014) Mitochondrial pathways and respiratory control. An introduction to OXPHOS analysis. 4th ed.
1429 Mitochondr Physiol Network 19.12. Oroboros MiPNet Publications, Innsbruck:80 pp.
1430 Gnaiger E, Méndez G, Hand SC (2000) High phosphorylation efficiency and depression of uncoupled respiration
1431 in mitochondria under hypoxia. Proc Natl Acad Sci USA 97:11080-5.
1432 Greggio C, Jha P, Kulkarni SS, Lagarrigue S, Broskey NT, Boutant M, Wang X, Conde Alonso S, Ofori E,
1433 Auwerx J, Cantó C, Amati F (2017) Enhanced respiratory chain supercomplex formation in response to
1434 exercise in human skeletal muscle. Cell Metab 25:301-11.
1435 Hinkle PC (2005) P/O ratios of mitochondrial oxidative phosphorylation. Biochim Biophys Acta 1706:1-11.
1436 Hofstadter DR (1979) Gödel, Escher, Bach: An eternal golden braid. A metaphorical fugue on minds and
1437 machines in the spirit of Lewis Carroll. Harvester Press:499 pp.
1438 Illaste A, Laasmaa M, Peterson P, Vendelin M (2012) Analysis of molecular movement reveals latticelike
1439 obstructions to diffusion in heart muscle cells. Biophys J 102:739-48.
1440 Jasienski M, Bazzaz FA (1999) The fallacy of ratios and the testability of models in biology. Oikos 84:321-26.

1441 Jepihhina N, Beraud N, Sepp M, Birkedal R, Vendelin M (2011) Permeabilized rat cardiomyocyte response
1442 demonstrates intracellular origin of diffusion obstacles. Biophys J 101:2112-21.
1443 Klepinin A, Ounpuu L, Guzun R, Chekulayev V, Timohhina N, Tepp K, Shevchuk I, Schlattner U, Kaambre T
1444 (2016) Simple oxygraphic analysis for the presence of adenylate kinase 1 and 2 in normal and tumor cells. J
1445 Bioenerg Biomembr 48:531-48.
1446 Klingenberg M (2017) UCP1 - A sophisticated energy valve. Biochimie 134:19-27.
1447 Koit A, Shevchuk I, Ounpuu L, Klepinin A, Chekulayev V, Timohhina N, Tepp K, Puurand M,Truu L, Heck K,
1448 Valvere V, Guzun R, Kaambre T (2017) Mitochondrial respiration in human colorectal and breast cancer
1449 clinical material is regulated differently. Oxid Med Cell Longev 1372640.
1450 Komlódi T, Tretter L (2017) Methylene blue stimulates substrate-level phosphorylation catalysed by succinyl-
1451 CoA ligase in the citric acid cycle. Neuropharmacology 123:287-98.
1452 Lane N (2005) Power, sex, suicide: mitochondria and the meaning of life. Oxford University Press:354 pp.
1453 Larsen S, Nielsen J, Neigaard Nielsen C, Nielsen LB, Wibrand F, Stride N, Schroder HD, Boushel RC, Helge
1454 JW, Dela F, Hey-Mogensen M (2012) Biomarkers of mitochondrial content in skeletal muscle of healthy
1455 young human subjects. J Physiol 590:3349-60.
1456 Lee C, Zeng J, Drew BG, Sallam T, Martin-Montalvo A, Wan J, Kim SJ, Mehta H, Hevener AL, de Cabo R,
1457 Cohen P (2015) The mitochondrial-derived peptide MOTS-c promotes metabolic homeostasis and reduces
1458 obesity and insulin resistance. Cell Metab 21:443-54.
1459 Lee SR, Kim HK, Song IS, Youm J, Dizon LA, Jeong SH, Ko TH, Heo HJ, Ko KS, Rhee BD, Kim N, Han J
1460 (2013) Glucocorticoids and their receptors: insights into specific roles in mitochondria. Prog Biophys Mol
1461 Biol 112:44-54.
1462 Leek BT, Mudaliar SR, Henry R, Mathieu-Costello O, Richardson RS (2001) Effect of acute exercise on citrate
1463 synthase activity in untrained and trained human skeletal muscle. Am J Physiol Regul Integr Comp Physiol
1464 280:R441-7.
1465 Lemieux H, Blier PU, Gnaiger E (2017) Remodeling pathway control of mitochondrial respiratory capacity by
1466 temperature in mouse heart: electron flow through the Q-junction in permeabilized fibers. Sci Rep 7:2840.
1467 Lenaz G, Tioli G, Falasca AI, Genova ML (2017) Respiratory supercomplexes in mitochondria. In: Mechanisms
1468 of primary energy trasduction in biology. M Wikstrom (ed) Royal Society of Chemistry Publishing, London,
1469 UK:296-337.
1470 Margulis L (1970) Origin of eukaryotic cells. New Haven: Yale University Press.
1471 Meinild Lundby AK, Jacobs RA, Gehrig S, de Leur J, Hauser M, Bonne TC, Flück D, Dandanell S, Kirk N,
1472 Kaech A, Ziegler U, Larsen S, Lundby C (2018) Exercise training increases skeletal muscle mitochondrial
1473 volume density by enlargement of existing mitochondria and not de novo biogenesis. Acta Physiol 222,
1474 e12905.
1475 Menshikova EV, Ritov VB, Fairfull L, Ferrell RE, Kelley DE, Goodpaster BH (2006) Effects of exercise on
1476 mitochondrial content and function in aging human skeletal muscle. J Gerontol A Biol Sci Med Sci 61:534-
1477 40.
1478 Menshikova EV, Ritov VB, Ferrell RE, Azuma K, Goodpaster BH, Kelley DE (2007) Characteristics of skeletal
1479 muscle mitochondrial biogenesis induced by moderate-intensity exercise and weight loss in obesity. J Appl
1480 Physiol (1985) 103:21-7.
1481 Menshikova EV, Ritov VB, Toledo FG, Ferrell RE, Goodpaster BH, Kelley DE (2005) Effects of weight loss
1482 and physical activity on skeletal muscle mitochondrial function in obesity. Am J Physiol Endocrinol Metab
1483 288:E818-25.
1484 Miller GA (1991) The science of words. Scientific American Library New York:276 pp.
1485 Mitchell P (1961) Coupling of phosphorylation to electron and hydrogen transfer by a chemi-osmotic type of
1486 mechanism. Nature 191:144-8.
1487 Mitchell P (2011) Chemiosmotic coupling in oxidative and photosynthetic phosphorylation. Biochim Biophys
1488 Acta Bioenergetics 1807:1507-38.
1489 Mogensen M, Sahlin K, Fernström M, Glintborg D, Vind BF, Beck-Nielsen H, Højlund K (2007) Mitochondrial
1490 respiration is decreased in skeletal muscle of patients with type 2 diabetes. Diabetes 56:1592-9.
1491 Mohr PJ, Phillips WD (2015) Dimensionless units in the SI. Metrologia 52:40-7.
1492 Moreno M, Giacco A, Di Munno C, Goglia F (2017) Direct and rapid effects of 3,5-diiodo-L-thyronine (T2).
1493 Mol Cell Endocrinol 7207:30092-8.
1494 Morrow RM, Picard M, Derbeneva O, Leipzig J, McManus MJ, Gouspillou G, Barbat-Artigas S, Dos Santos C,
1495 Hepple RT, Murdock DG, Wallace DC (2017) Mitochondrial energy deficiency leads to hyperproliferation of
1496 skeletal muscle mitochondria and enhanced insulin sensitivity. Proc Natl Acad Sci U S A 114:2705-10.
1497 Paradies G, Paradies V, De Benedictis V, Ruggiero FM, Petrosillo G (2014) Functional role of cardiolipin in
1498 mitochondrial bioenergetics. Biochim Biophys Acta 1837:408-17.
1499 Pesta D, Gnaiger E (2012) High-Resolution Respirometry. OXPHOS protocols for human cells and
1500 permeabilized fibres from small biopsies of human muscle. Methods Mol Biol 810:25-58.
1501 Pesta D, Hoppel F, Macek C, Messner H, Faulhaber M, Kobel C, Parson W, Burtscher M, Schocke M, Gnaiger
1502 E (2011) Similar qualitative and quantitative changes of mitochondrial respiration following strength and

1503 endurance training in normoxia and hypoxia in sedentary humans. Am J Physiol Regul Integr Comp Physiol
1504 301:R1078–87.
1505 Price TM, Dai Q (2015) The role of a mitochondrial progesterone receptor (PR-M) in progesterone action.
1506 Semin Reprod Med 33:185-94.
1507 Puchowicz MA, Varnes ME, Cohen BH, Friedman NR, Kerr DS, Hoppel CL (2004) Oxidative phosphorylation
1508 analysis: assessing the integrated functional activity of human skeletal muscle mitochondria – case studies.
1509 Mitochondrion 4:377-85. Puntschart A, Claassen H, Jostarndt K, Hoppeler H, Billeter R (1995) mRNAs of
1510 enzymes involved in energy metabolism and mtDNA are increased in endurance-trained athletes. Am J
1511 Physiol 269:C619-25.
1512 Quiros PM, Mottis A, Auwerx J (2016) Mitonuclear communication in homeostasis and stress. Nat Rev Mol
1513 Cell Biol 17:213-26.
1514 Reichmann H, Hoppeler H, Mathieu-Costello O, von Bergen F, Pette D (1985) Biochemical and ultrastructural
1515 changes of skeletal muscle mitochondria after chronic electrical stimulation in rabbits. Pflugers Arch 404:1-
1516 9.
1517 Renner K, Amberger A, Konwalinka G, Gnaiger E (2003) Changes of mitochondrial respiration, mitochondrial
1518 content and cell size after induction of apoptosis in leukemia cells. Biochim Biophys Acta 1642:115-23.
1519 Rich P (2003) Chemiosmotic coupling: The cost of living. Nature 421:583.
1520 Rostovtseva TK, Sheldon KL, Hassanzadeh E, Monge C, Saks V, Bezrukov SM, Sackett DL (2008) Tubulin
1521 binding blocks mitochondrial voltage-dependent anion channel and regulates respiration. Proc Natl Acad Sci
1522 USA 105:18746-51.
1523 Rustin P, Parfait B, Chretien D, Bourgeron T, Djouadi F, Bastin J, Rötig A, Munnich A (1996) Fluxes of
1524 nicotinamide adenine dinucleotides through mitochondrial membranes in human cultured cells. J Biol Chem
1525 271:14785-90.
1526 Saks VA, Veksler VI, Kuznetsov AV, Kay L, Sikk P, Tiivel T, Tranqui L, Olivares J, Winkler K, Wiedemann F,
1527 Kunz WS (1998) Permeabilised cell and skinned fiber techniques in studies of mitochondrial function in
1528 vivo. Mol Cell Biochem 184:81-100.
1529 Salabei JK, Gibb AA, Hill BG (2014) Comprehensive measurement of respiratory activity in permeabilized cells
1530 using extracellular flux analysis. Nat Protoc 9:421-38.
1531 Sazanov LA (2015) A giant molecular proton pump: structure and mechanism of respiratory complex I. Nat Rev
1532 Mol Cell Biol 16:375-88.
1533 Schneider TD (2006) Claude Shannon: biologist. The founder of information theory used biology to formulate
1534 the channel capacity. IEEE Eng Med Biol Mag 25:30-3.
1535 Schönfeld P, Dymkowska D, Wojtczak L (2009) Acyl-CoA-induced generation of reactive oxygen species in
1536 mitochondrial preparations is due to the presence of peroxisomes. Free Radic Biol Med 47:503-9.
1537 Schultz J, Wiesner RJ (2000) Proliferation of mitochondria in chronically stimulated rabbit skeletal muscle--
1538 transcription of mitochondrial genes and copy number of mitochondrial DNA. J Bioenerg Biomembr 32:627-
1539 34.
1540 Simson P, Jepihhina N, Laasmaa M, Peterson P, Birkedal R, Vendelin M (2016) Restricted ADP movement in
1541 cardiomyocytes: Cytosolic diffusion obstacles are complemented with a small number of open mitochondrial
1542 voltage-dependent anion channels. J Mol Cell Cardiol 97:197-203.
1543 Stucki JW, Ineichen EA (1974) Energy dissipation by calcium recycling and the efficiency of calcium transport
1544 in rat-liver mitochondria. Eur J Biochem 48:365-75.
1545 Tonkonogi M, Harris B, Sahlin K (1997) Increased activity of citrate synthase in human skeletal muscle after a
1546 single bout of prolonged exercise. Acta Physiol Scand 161:435-6.
1547 Waczulikova I, Habodaszova D, Cagalinec M, Ferko M, Ulicna O, Mateasik A, Sikurova L, Ziegelhöffer A
1548 (2007) Mitochondrial membrane fluidity, potential, and calcium transients in the myocardium from acute
1549 diabetic rats. Can J Physiol Pharmacol 85:372-81.
1550 Wagner BA, Venkataraman S, Buettner GR (2011) The rate of oxygen utilization by cells. Free Radic Biol Med
1551 51:700-712.
1552 Wang H, Hiatt WR, Barstow TJ, Brass EP (1999) Relationships between muscle mitochondrial DNA content,
1553 mitochondrial enzyme activity and oxidative capacity in man: alterations with disease. Eur J Appl Physiol
1554 Occup Physiol 80:22-7.
1555 Watt IN, Montgomery MG, Runswick MJ, Leslie AG, Walker JE (2010) Bioenergetic cost of making an
1556 adenosine triphosphate molecule in animal mitochondria. Proc Natl Acad Sci U S A 107:16823-7.
1557 Weibel ER, Hoppeler H (2005) Exercise-induced maximal metabolic rate scales with muscle aerobic capacity. J
1558 Exp Biol 208:1635–44.
1559 White DJ, Wolff JN, Pierson M, Gemmell NJ (2008) Revealing the hidden complexities of mtDNA inheritance.
1560 Mol Ecol 17:4925–42.
1561 Wikström M, Hummer G (2012) Stoichiometry of proton translocation by respiratory complex I and its
1562 mechanistic implications. Proc Natl Acad Sci U S A 109:4431-6.
1563 Willis WT, Jackman MR, Messer JI, Kuzmiak-Glancy S, Glancy B (2016) A simple hydraulic analog model of
1564 oxidative phosphorylation. Med Sci Sports Exerc 48:990-1000.